pubs.acs.org/Biomac

Article

Analysis of Cytoplasmic and Membrane Molecular Crowding in Genetically Programmed Synthetic Cells

David Garenne* and Vincent Noireaux*

Cite This: https://dx.doi.org/10.1021/acs.biomac.0c00513

Read Online

ACCESS | Metrics & More | Article Recommendations | Supporting Information

ABSTRACT: Building genetically programmed synthetic cell systems by molecular integration is a powerful and effective approach to capture the synergies between biomolecules when they are put together. In this work, we characterized quantitatively the effects of molecular crowding on gene expression in the cytoplasm of minimal cells, when a crowding agent is added to the reaction, and on protein self-assembly at the membrane, when a crowding agent is attached to the lipid bilayer. We demonstrate that achieving membrane crowding only is sufficient to keep cytoplasmic expression at its highest and to promote the polymerization of the MreB cytoskeletal protein at the lipid bilayer into a network that is mechanically sturdy. Furthermore, we show that membrane crowding can be emulated by different types of macromolecules, supporting a purely entropic mode of action for supramolecular assembly of cytoskeletal proteins at the bilayer. These unanticipated results provide quantitative and general insights relevant to synthetic cell builders.

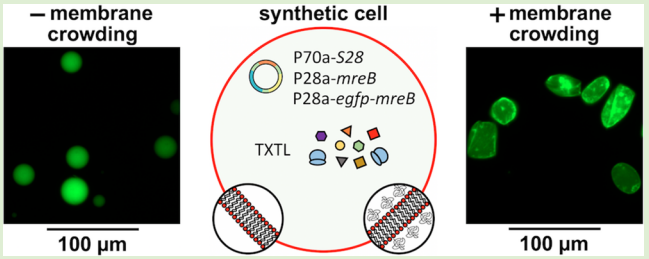

1. INTRODUCTION

The bottom-up synthesis of cell-sized compartments that are programmed genetically for specific biological functions has become a central approach to building biologically active cell analogs.[1−3] The foremost experimental scheme consists of encapsulating a cell-free transcription−translation (TXTL) reaction into liposomes.[4−12] This approach allows executing gene circuits in isolation without genomic information in the background. The goals of assembling synthetic cells from scratch are both fundamental and applied.[13] At the basic level, building minimal cells enables a deeper comprehension of the synergies that arise when biomolecules are put together at a relevant biological scale. On a broader scope, the objective is to develop a better understanding of how to integrate into a functioning synthetic cell the three essential molecular blocks: information, metabolism, and compartment.[14,15] Working in a minimal cell setting has gained substantial credibility and popularity in the last years because such analysis facilitates dissociating complex processes that are often entangled in vivo.

A TXTL system has many advantages for building synthetic cells by molecular integration. A cell-free reaction contains the natural biomacromolecules for transcription (RNA polymerase) and translation (ribosomes), as well as all the necessary building blocks (amino acids and ribonucleosides) to sustain DNA-dependent protein synthesis for several hours. By recapitulating gene expression in vitro, TXTL enables programming minimal cells with natural or synthetic gene circuits.[16−21] A typical cell-free reaction based on a cytoplasmic extract contains about 10 mg/mL of proteins, which corresponds to a 25−30× dilution compared to the concentration of proteins found in the cytoplasm of a bacterium like *E. coli* (∼250−300 mg/mL of protein). To emulate the high density of macromolecules found in living cells and thus increase the efficacy of transcription and translation in vitro, molecular crowders are added to TXTL reactions. This method is well established in the field of cell-free gene expression and, to a larger extent, for biochemical reactions performed in vitro.[22] Most of the TXTL platforms contain a few millimolar of crowders, such as polyethylene glycol (PEG), Ficoll, or Dextran.[23−25] For instance, PEG of molecular mass 8000 g/mol can increase cell-free protein synthesis several folds in either test tube reactions or liposomes.[26,27] While adding a crowding agent to cell-free expression mixtures is a well-known procedure to increase the effective concentrations of the reaction components, some other biophysical consequences of high concentrations of biomacromolecules similar to the ones found in living cells have been less studied in minimal cell systems. In particular, it is known that the self-assembly of cytoskeletal proteins is promoted by molecular crowding.[28,29] Recently, we showed that emulating molecular crowding specifically at the lipid bilayer of synthetic cells has a considerable effect on the polymerization of cytoskeletal proteins interacting with the membrane.[30] The assembly of

Received: April 7, 2020
Revised: May 21, 2020
Published: May 22, 2020

the *E. coli* protein MreB at the inner membrane of synthetic cells into an active cytoskeleton network capable of deforming spherical liposomes into rods is dramatically increased in the presence of PEG molecules attached to the lipid bilayer, independent of the presence or not of a crowder in the reaction.

In this work, we report a quantitative analysis of the effects of membrane (two-dimensional) and cytoplasmic (three-dimensional) molecular crowding on the synthesis of soluble proteins in the cytoplasm and on the self-assembly of the MreB protein at the membrane of TXTL-based minimal cells. Several new and unexpected results emerge from our observations. On a general standpoint, emulating molecular crowding at the membrane of synthetic cells, using a lipid-PEG, offers all the advantages. First, adding a molecular crowder to the cytoplasm of a minimal cell is unnecessary when molecular crowding is achieved at the membrane. We observe that cell-free expression of reporter genes is optimum in minimal cells when lipid-PEGs are used without adding PEG to the reaction. In these conditions, the final concentration of a dynamically synthesized reporter protein is identical over a liposome population of radii from 0.5 to 15 μm. Second, when membrane molecular crowding is carried out using lipid-PEGs, the number of minimal cells formed using the emulsion method[31,32] increases by a factor of 10 on average. Third, two-dimensional molecular crowding at the membrane can be achieved by different biopolymers. The *E. coli* protein MreB, a prokaryotic actin homologue, spontaneously self-assemble into a sturdy filament network when either PEG or biotin-binding proteins are attached to the membrane, thus, providing several ways to emulate membrane crowding, all experimentally easy to implement. As importantly, this observation shows that the presence of a background of biomacromolecules attached to the membrane is responsible for stimulating the self-assembly of MreB, thus, supporting the hypothesis that this mechanism is entropically driven. While the synthesis of MreB and reporter proteins do not capture all the aspects of molecular crowding, the results obtained with these proteins provide minimal cell builders with tools and quantitative measurements that will facilitate emulating biological functions reconstituted in genetically programmed synthetic cells. The observations are also relevant to the biophysics of living cells.

2. EXPERIMENTAL SECTION

Materials. Lipids were purchased from Avanti Polar Lipids Inc. (Alabaster, AL): egg PC (#131601), PE-PEG5000 (#880200), PE-PEG2000 (#880160), and Biotinyl cap PE (#870277). Avidin (Fisher, #A2667), molecular mass of 66−69 kDa, is highly glycosylated, with about 10% of its total mass being carbohydrates. The isoelectric point of avidin is 10−10.5, which makes it positively charged in cell-free reactions of pH 8. Neutravidin (VWR, #PI31000), molecular mass of 60 kDa, is a deglycosylated form of avidin. The isoelectric point of neutravidin is 6.3, which makes it negatively charged in cell-free reactions. Streptavidin (VWR, PI21125), with a molecular mass of 55 kDa, has an isoelectric point of 5, which makes it negatively charged in cell-free reactions. The similarity between the amino sequences of avidin and streptavidin is on the order of 25% only.

DNA Constructs. The sequences of the coding parts of the DNA constructs used in this work are reported in the Table S1. All the constructs have been sequenced and were prepared using standard cloning procedures. The plasmids P70a-*degfp* and P70a-*mcherry* have been described previously.[18] The reporter protein deGFP (25.4 kDa, 1 mg/mL = 39.4 μM) is a slightly truncated version of eGFP with the same fluorescent properties as eGFP. The plasmid P70a-*S28* has been described earlier.[33] The plasmids P28a-*mreB* and P28a-*egfp-mreB* have been described in ref 30. All the DNA constructions are available at Arbor Biosciences (Toolbox 2.0 Plasmid Collection).

TXTL System. The kit myTXTL (Arbor Biosciences, #507024) was used for cell-free expression. This experimental platform has been described previously,[26,33,34] its capabilities have been reported thoroughly,[18] and its protein composition was determined by mass spectrometry in a recent article.[35] The molecular components necessary for transcription consist of the *E. coli* core RNA polymerase and sigma factor 70. Other RNA polymerases or transcription factors with their specific promoters, such as the T7 RNA polymerase or the sigma factor 28, can be used by executing transcriptional activation cascades, as reported before.[18,33] TXTL reactions are composed of an *E. coli* lysate, an amino acid mixture, and an energy buffer, to which the desired DNA templates are added. The concentration of the plasmid P28a-*egfp-mreB* was systematically set to 10% of the concentration of P28a-*mreB* (e.g., 2 nM P28a-*mreB*, 0.2 nM P28a-*egfp-mreB*). All the reactions (batch mode, liposomes) were incubated at 29 °C in either a benchtop incubator, for end point measurements, or in the plate readers, for kinetic measurements. The optimum temperature of incubation for the myTXTL kit is 29 °C.

Batch Mode Reactions. Batch mode TXTL reactions were prepared on a Labcyte Echo liquid dispenser, in 2 μL volumes, on sealed polypropylene 96-well V-bottom plates (Sigma #CLS3357, Sigma #CLS3080). For kinetics, the fluorescence was measured at 3 min intervals using monochromators (deGFP: Ex/Em 488/525 nm, mCherry: Ex/Em 580/615 nm) on a Biotek Synergy H1m plate reader. End-point reactions were measured after 12 h of incubation. To measure protein concentration (eGFP), a linear calibration curve of fluorescence intensity versus eGFP concentration was generated using purified recombinant eGFP obtained from Cell Biolabs, Inc. (#STA-201). Recombinant mCherry was obtained from Origene (#TP790040), from which a linear calibration curve of fluorescence intensity versus mCherry concentration was generated for quantification.

Liposome Preparation. The preparation of TXTL-loaded liposomes, based on the emulsion method,[31] has been described in detail by our group in a recent publication.[32] Briefly, the phospholipids were dissolved in chloroform at a concentration around 20 mg/mL. The lipids were added to mineral oil at a concentration of 2 mg/mL and incubated for 1 h at 80 °C to evaporate the chloroform. A total of 5 μL of TXTL reaction was added to 500 μL of mineral oil lipid mix, followed by a gentle vortex for a few seconds to create an emulsion. A total of 200 μL of the emulsion was placed on top of 50 μL of feeding solution; this solution was centrifuged for 1 min at 5000 g. The liposome solution was recovered and placed on a microscope cover glass, sealed, and allowed to incubate at 29 °C. The osmolarity of TXTL reactions and of the external solution was estimated using an osmometer Advanced Instrument 3320. All the lipid mixtures are given in % molar. For instance, 98% PC + 2% lipid-biotin means that out of 100 phospholipids, 98 are PC and 2 are lipid-biotin.

Imaging and Data Analysis. Fluorescence images of liposomes were taken on an inverted microscope Olympus IX-81 connected to an Andor iXon3 CCD camera. The images were acquired in focus with a 40x objective, with a depth of field of 1 μm, and the intensity was integrated over the fluorescence disc and background subtracted. The light intensity was moderate so as to work in the linear response of the camera and prevent photobleaching. Images analysis (fluorescence intensity and L/S ratio measurements) were carried out using MetaMorph (Molecular Devices). At least 20 liposomes were analyzed for each condition, with radii between 0.5 and 15 μm. The error bars in the histograms indicate the standard deviation of three independent repeats. An independent repeat consisted of preparing a synthetic cell solution from scratch, using new aliquots of materials. Histograms were obtained from the scattered plots.

Data and Code Availability. Data are available upon request.

3. RESULTS AND DISCUSSION

Cell-Free and Minimal Cell Systems. The TXTL system used in this work is the commercially available kit myTXTL

https://dx.doi.org/10.1021/acs.biomac.0c00513
Biomacromolecules XXXX, XXX, XXX−XXX

(Arbor Biosciences). The reporter genes were expressed either from the *E. coli* constitutive promoter P70a or P28a through a transcriptional activation cascade. The cytoskeleton proteins MreB were synthesized from the sigma 28 transcriptional cascade that enables the expression of genes toxic to *E. coli* through the silent promoter P28a (Figure S1). The maximum protein synthesis yield in batch mode is 3 mg/mL for the fluorescent reporter deGFP,[30] which corresponds to about 115−120 μM.

In TXTL reactions, several different molecular crowders are suitable for emulating the large concentrations of macromolecules found in living cells, and thus for accelerating reaction rates and increasing protein synthesis. PEG, Ficoll, and Dextran are the most popular crowders.[23−25] In this work, our standard bulk crowding agent was PEG8000, at a concentration of 1.5−2.5 mM. A PEG of molecular mass of 8000 g/mol is optimum for cell-free expression for the system used in this work. This polymer is highly compatible with TXTL reactions and has the advantage to be nonionic. It is easy to set its concentration in a broad range (0−10 mM). As importantly, the other reason for choosing PEG is that only phospholipid-PEG is commercially available for membrane crowding (Dextran or Ficoll lipids are not commercially available).

The batch mode reactions are executed in test tubes or on well plates and analyzed on plate readers (Figure 1). The quantitative

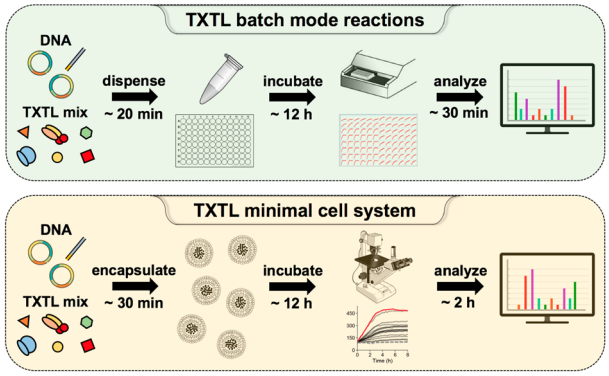

Figure 1. Overview of the TXTL experiments carried out in test tubes or in synthetic cells. In batch mode, the reactions are typically performed on well plates incubated on a plate reader for kinetics and in an incubator for end points. Reactions can also be performed in 1.5 mL test tubes and added to a well plate for signal measurements. Minimal cells are observed under a microscope by fluorescence. In both cases, TXTL reactions last up to 10−12 h before reaching a plateau after the resources (ATP, GTP, amino acids) have been consumed.

measurements using deGFP or mCherry were determined from linear calibrations of the plate readers based on purified recombinant reporter proteins as described before.[18] The minimal cell system is made by encapsulating a cell-free reaction into cell-sized liposomes, following a procedure described previously[31] and optimized for cell-free expression reactions[32] (Figure 1). The method employed has several advantages: it is fast, liposomes are prepared in about 15−30 min, the encapsulation efficiency is high,[36] and the number of phospholipid vesicles produced is large. Several tens of liposomes are visible in a single field of view when observed under a microscope with a 40× objective. In this work we expressed two reporter genes, *degfp* and *mcherry*. The protein deGFP is a slightly modified version of eGFP with the same respective fluorescent properties.[33] We chose deGFP and mCherry because their amino acid sequences are unrelated and are less than 30% identical when aligned.

Effects of Two- and Three-Dimensional Molecular Crowding on the Synthesis of Soluble Reporter Proteins in Minimal Cells. The first goal of our study was to characterize the effects of membrane and of cytoplasmic molecular crowding on the synthesis of soluble fluorescent proteins. We used phospholipid-PEGs (PE−PEG; Table S2) to emulate membrane crowding, as they are commercially available in several sizes for the PEG moiety. We used a PE-PEG5000 for membrane crowding, as reported before.[30] We analyzed the four cases possible: (i) no PEG8000 in solution, no PE-PEG5000 in the membrane, (ii) PEG8000 in solution, no PE-PEG5000 in the membrane, (iii) no PEG8000 in solution, PE-PEG5000 in the membrane, (iv) PEG8000 in solution, PE-PEG5000 in the membrane. This set was performed separately for two different reporter genes: *degfp* and *mcherry* (Table S1). In our previous studies, we demonstrated that the optimum PEG8000 concentration is around 1.5−2.5% (1.875−3.125 mM).[18,33] We fixed PEG8000 to 1.5% when it was added to a TXTL reaction. Recently, we showed that a membrane concentration of 0.5−1% molar of PE-PEG5000 is optimum for the self-assembly of MreB.[30] The reason for this is related to the coverage of the membrane by the PEG molecule. In the case of PE-PEG5000, full coverage of the membrane by the PEG molecules occurs around 1%. Thus, at larger PE-PEG5000 concentrations, the interactions of membrane-interacting proteins with the bilayer are screened (Table S2). We fixed the molar concentration of PE-PEG5000 to 0.66% when it was used, with 99.33% PC.

First, we encapsulated pure fluorescent proteins into liposomes with or without PEG8000 added to the reaction and with or without PE-PEG5000 in the membrane so as to determine, in the four cases, the response of fluorescence intensity with respect to the geometry of the system, consisting of spherical liposomes. We used standard one photon fluorescence microscopy. Populations of 20 to 200 spherical liposomes were analyzed for each of the four cases, with radii between 0.5 and 15 μm. The fluorescence intensity was plotted with respect to the square of the radius. For deGFP, in all the cases, the fluorescence intensity across the liposome population is linear with respect to the square of the liposomes' radii (Figure 2). This result indicates that the encapsulation process of the cell-free system is homogeneous and uniform. While the fits are quantitatively close for the four cases, the one with PE-PEG5000 in the membrane is slightly greater. The same observations can be made when mCherry was encapsulated in liposomes. Taken together, this method tells us that the encapsulation of the extract components (the proteins of the lysate) into cell-sized liposomes is rather homogeneous independently of whether cytoplasmic and membrane crowders are carried out.

Our next experiment consisted of expressing *degfp* from the *E. coli* constitutive promoter P70a inside the liposomes for the same four cases (Figure 3). Three major outcomes emerged from the observations when deGFP was synthesized in the presence or absence of either PEG8000 in solution or PE-PEG5000 at the membrane. First, deGFP synthesis is largest in liposomes when only the lipid-PEG is added to the membrane, without PEG8000 in solution. The fact that the effect of cytoplasmic crowding vanishes in the presence of membrane crowding was unexpected. Because PEG polymers are known to prevent nonspecific adsorption on surfaces, this result indicates that the interactions of the reaction components with the

https://dx.doi.org/10.1021/acs.biomac.0c00513
Biomacromolecules XXXX, XXX, XXX−XXX

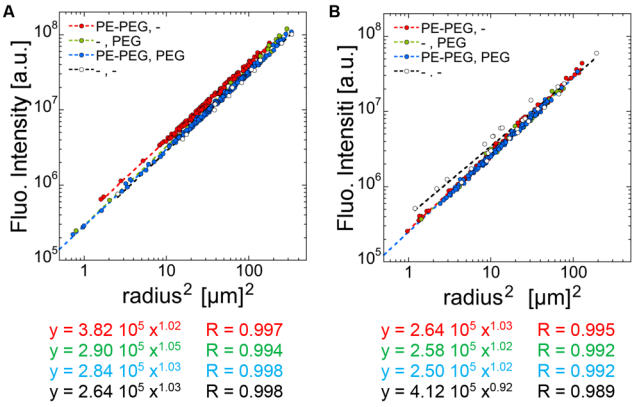

Figure 2. Encapsulation of pure eGFP or pure mCherry into liposomes. eGFP or mCherry was added to a standard cell-free reaction containing all the components except DNA templates. Four types of liposome population were prepared, with or without 0.66% DSPE-PEG5000 in the membrane and with or without PEG8000 in the solution. The blank case is without both (100% PC membrane). Fluorescence intensity was measured on a microscope using a 40× objective for populations of cell-sized liposomes with radii from 0.5 to 15 μm. (A) For eGFP, the intensity is linear with respect to the square of the liposomes' radii (power fit) in the four cases. There is no major difference in the magnitude of the intensity between the four cases. (B) For mCherry, the blank case is not linear. The three other cases are linear with respect to the square of the liposomes' radii (power fit).

membrane dominate the behavior of cell-free protein synthesis in liposomes. In that particular case, interactions of some reaction components are detrimental to protein synthesis in the absence of PEG at the membrane. Second, it is also when only the PE-PEG5000 is added to the minimal cell system that the response is the most linear and shows the least fluctuations in protein synthesis among the liposome population. Third and last, the number of liposomes produced increases by a factor of about 10 when the lipid-PEG is used, independent of the presence of PEG8000 in the reaction. Hence, adding a lipid-PEG to the membrane has many advantages, without noticeable downsides. When the PE-PEG5000 (0.66%) is replaced by PE-PEG2000 (1%; Table S2), the observations are qualitatively similar, although two noticeable differences appear (Figure S2). First, the case with both crowding is comparable to the case with membrane crowding only. The case with membrane crowding only is not as linear as when PE-PEG5000 is used. Consequently, membrane crowding is more effective with the PE-PEG5000. These results obtained with PE-PEG5000 indicate that the presence of PEG attached to the membrane enables a homogeneous encapsulation of the TXTL reaction inside the liposomes and that the concentration of deGFP produced in the liposomes is constant over the size range (0.5−15 μm radius).

When mCherry is dynamically synthesized into the liposomes from the same promoter and in the same conditions, the major trends observed for deGFP are conserved, although slight differences are observed (Figure S3). The smallest protein synthesis yield is observed when no crowding at all is used, a case that also shows the largest fluctuations in a single population of liposomes. The synthesis of mCherry in the minimal cells for the three other conditions is similar. The case with only the

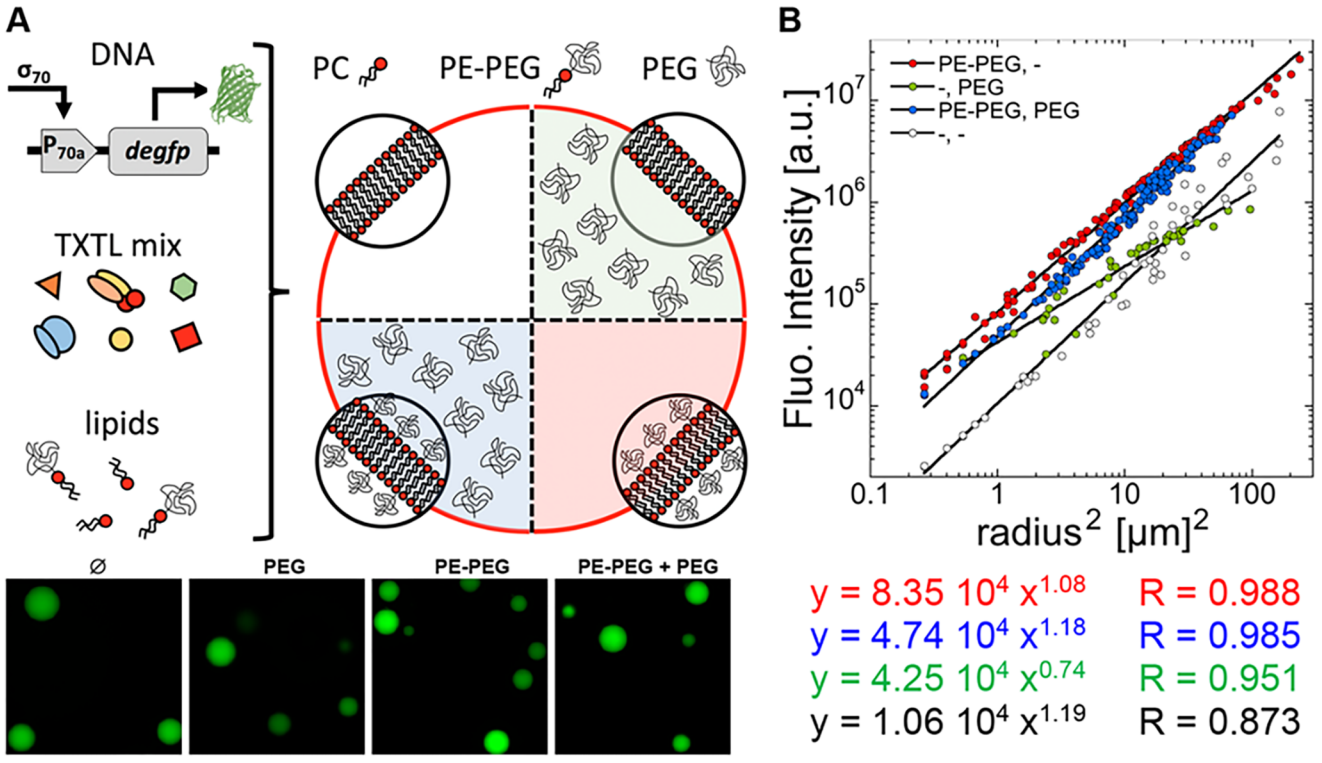

Figure 3. Cell-free expression of *degfp* in synthetic cells in the presence or absence of PEG8000 (noted PEG) in the reaction and DSPE-PEG5000 (noted PE-PEG) at the membrane. (A) The reaction components are encapsulated in cell-sized liposomes to express *degfp* through the P70a constitutive promoter (plasmid P70a-*degfp*, 5 nM). Four types of liposome populations are made with PEG and PE-PEG, with PEG only, with PE-PEG only, and with none. The fluorescence images are acquired after 12 h of incubation. Each image is a square of 100 μm. (B) The fluorescence intensity is plotted with respect to the square of the radius of the liposomes and power fitted.

https://dx.doi.org/10.1021/acs.biomac.0c00513
Biomacromolecules XXXX, XXX, XXX−XXX

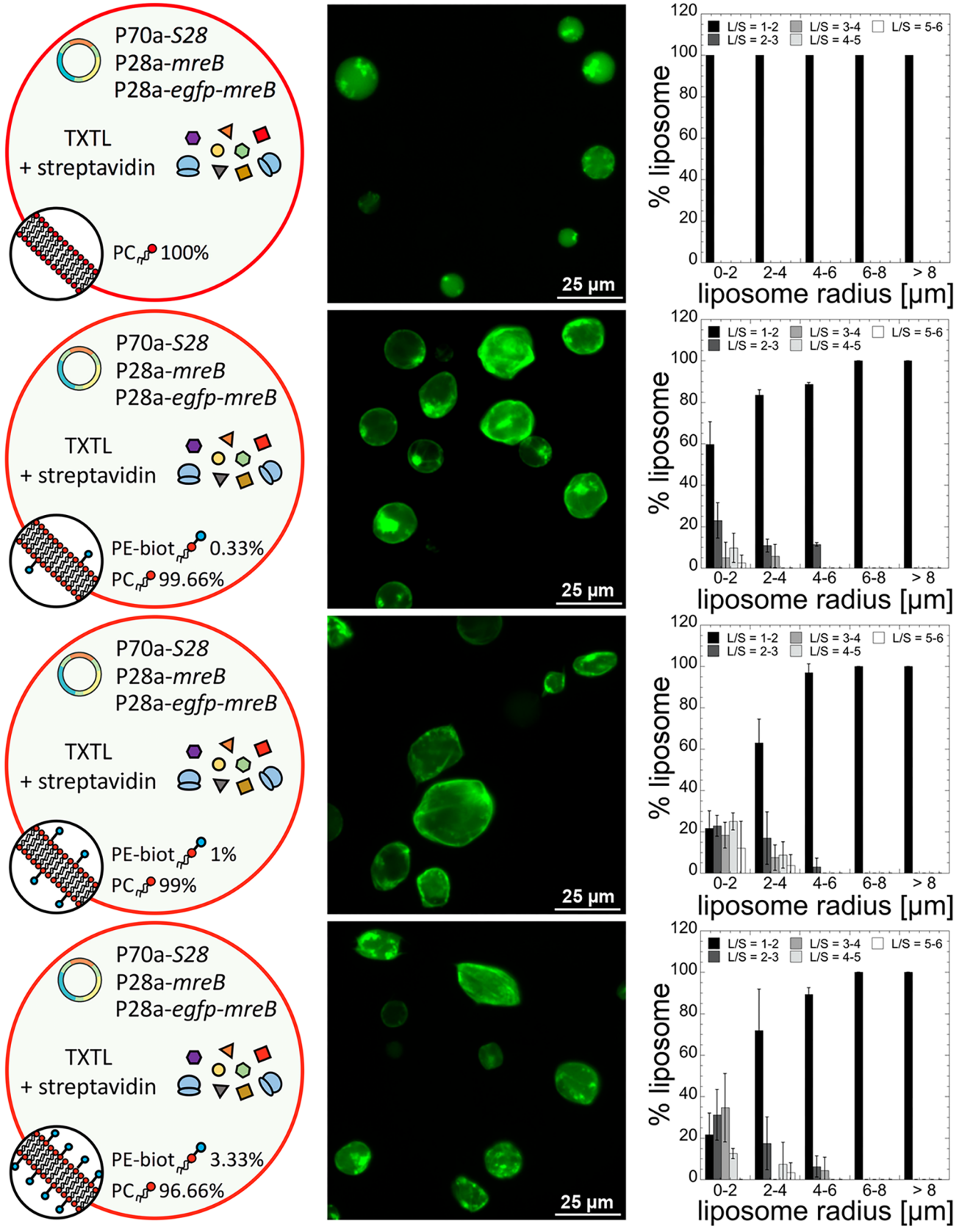

Figure 4. Statistics of liposome deformation (ratio *L*/*S*, long axis over short axis) as a function of the concentration of lipid PE-biotin (noted as PE-biot) in the membrane. The bilayer of the synthetic cells is composed of egg PC with either 0%, 0.33%, 1%, and 3.33% of PE-biot (% indicates molarity). Streptavidin was added to the reaction at a concentration of 20 μM in all the cases. No deformation is observed when *mreB* is expressed without PE-biot in the membrane (0.5 nM P70a-*S28*, 2 nM P28a-*mreB*, 0.2 nM P28a-*egfp-mreB*). The statistics of deformation are the most pronounced for 1% PE-biot in the membrane. The liposomes' radii are the radii measured before deformation when liposomes are all spherical.

https://dx.doi.org/10.1021/acs.biomac.0c00513
Biomacromolecules XXXX, XXX, XXX−XXX

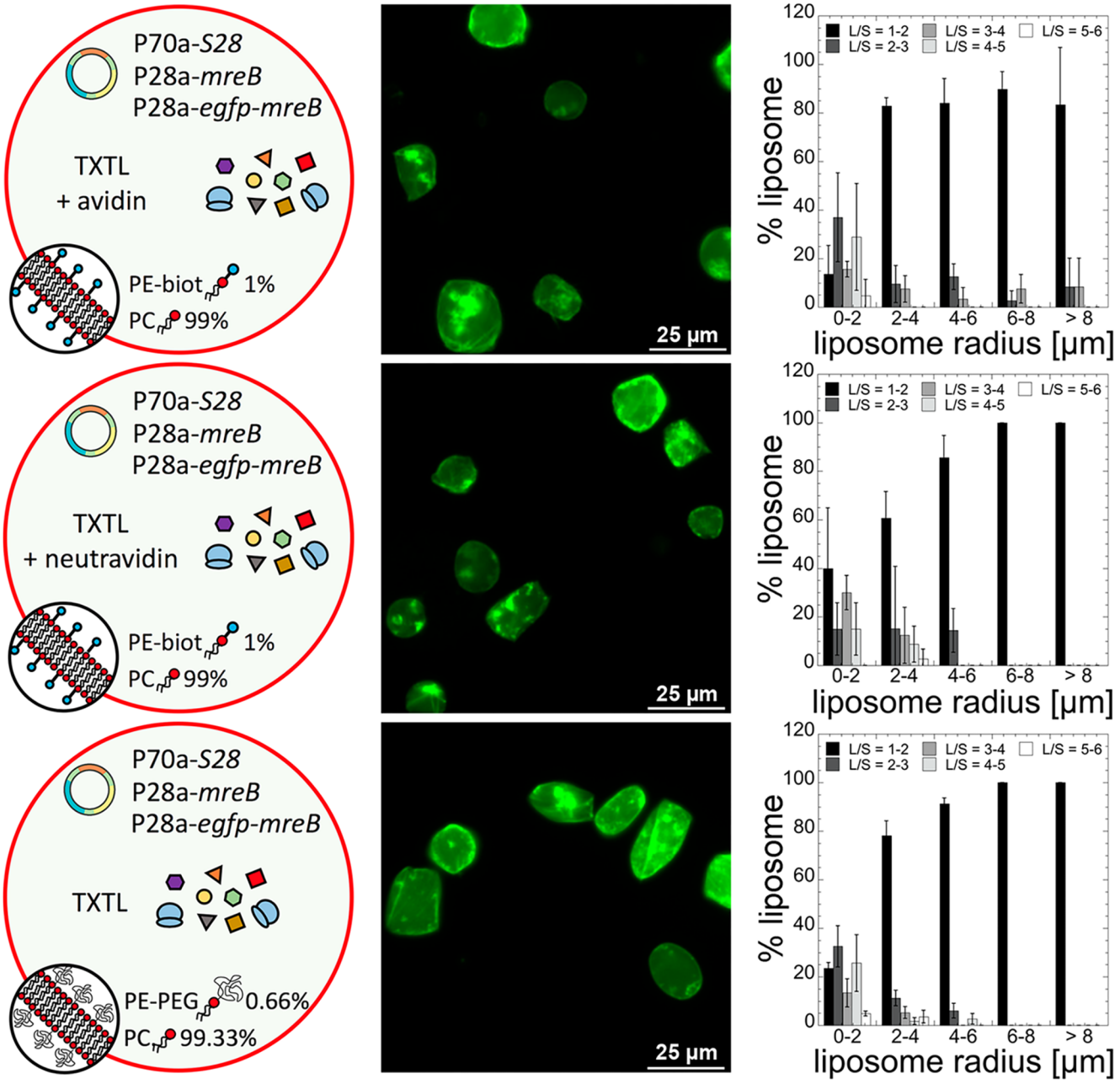

Figure 5. Statistics of liposome deformation (ratio L/S, long axis over short axis) as a function of the presence of one of three different macromolecules at the membrane: avidin, neutravidin or PEG5000 in the membrane. In the case of avidin and neutravidin (20 μM added to the reaction), the bilayer of the synthetic cells is composed of 99% egg PC and 1% lipid-biotin. In the case of PEG5000, the bilayer of the synthetic cells is composed of 99.33% egg PC and 0.66% PE-PEG5000. Plasmid concentrations: 0.5 nM P70a-*S28*, 2 nM P28a-*mreB*, and 0.2 nM P28a-*egfp-mreB*. Similar statistics of deformation are observed, comparable to the use of streptavidin (Figure 4).

membrane crowding, however, shows the most linear response in terms of protein synthesis. This results strengthen the conclusion that implementing membrane crowding only with PE-PEG5000 is sufficient to achieve the optimum protein synthesis in minimal cell systems and a linear response with respect to the size of the liposomes. We hypothesize that the differences observed between the encapsulation experiment (pure fluorescent proteins) and the dynamic synthesis of the reporter proteins are due to two factors: the heterogeneity in the encapsulation of the DNA template (the largest molecule and smallest concentration in a TXTL reaction), as studied before,[37] and the effect of the membrane surface on gene expression, as shown previously.[38] In any case, we observe that adding PE-PEG5000 to the membrane reduces to negligible levels the fluctuations due to these factors, so that cell-free protein synthesis in cell-sized liposomes (1−30 μm diameter) is uniform and at its optimum.

Effects of Membrane and Cytoplasmic Molecular Crowding on the Self-Assembly of the MreB Protein. We recently evidenced that molecular crowding at the membrane dramatically accelerates the self-assembly of the *E. coli* MreB protein at the bilayer into a cytoskeleton network sturdy enough to change spherical minimal cells into rods.[30] We determined that cytoplasmic molecular crowding has no effect in

https://dx.doi.org/10.1021/acs.biomac.0c00513
Biomacromolecules XXXX, XXX, XXX−XXX

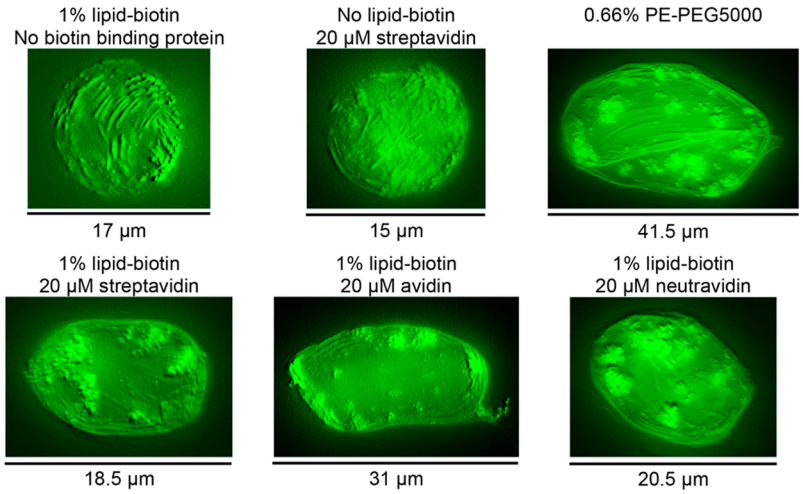

Figure 6. 3D reconstruction of liposomes expressing *mreB* as a function of the membrane composition and the addition of biotin-binding proteins. The membranes were composed of PC and the indicated lipid. Plasmid concentrations: 0.5 nM P70a-*S28*, 2 nM P28a-*mreB*, and 0.2 nM P28a-*egfp-mreB*. A net accumulation of MreB filaments is observed when membrane crowding is observed. One can also observe a few filaments at the membrane of undeformed liposomes. Some filament bundles are stretching the membrane (0.66% PE-PEG5000 and avidin cases). This phenotype is observed in all the membrane crowding cases. Some aggregates of MreB are also observed, mostly when membrane crowding is present, as reported before.[30]

this process. A major question to address is whether this result is limited and specific to PEG or do other biomacromolecules attached to the membrane produce the same effect? The latter case would support that entropy is responsible for promoting and accelerating the self-assembly of MreB at the membrane, independent of the type of macromolecules attached to the bilayer.

In order to emulate molecular crowding at the membrane other than using PE-PEG lipids, we used the biotin−streptavidin system, which consisted of adding a biotinylated lipid to the membrane and streptavidin to the reaction. The biotin−streptavidin system has several advantages: it is well-established, the interaction is highly specific and strong, it enables emulating crowding at the membrane with molecules that have a completely different chemical composition compared to PEG. We also tested two streptavidin analogs: avidin and neutravidin. The three biotin-binding proteins have comparable molecular masses, but different isoelectric points and, thus, different charges in cell-free reactions of pH 8 (see methods details). In addition, streptavidin has only 25% amino acid sequence similarity with avidin and neutravidin. Streptavidin is a tetramer of depth 2−2.5 nm and diameter 11 nm when attached to a surface.[39] Taking a surface area of about 100 nm^2, we find that for a liposome of radius 5 μm, a concentration of 10 μM streptavidin is needed to cover the whole liposome inner membrane. Considering the large biotin−streptavidin affinity ($K_A = 10^{14}$ M^{-1}),[39] liposome sizes of a few micrometers, and a diffusion coefficient around 50 $\mu m^2/s$ (Stokes−Einstein), we find that it takes about 0.1 s for a protein of the size of streptavidin to travel across a liposome. Therefore, the process of streptavidin adsorption onto the inner membrane reaches equilibrium in just a few minutes, before the synthesis of MreB starts, which takes about 30 min using the S28 transcriptional activation cascade (Figure S1). The synthesis of MreB and eGFP-MreB is optimum at a plasmid concentration of 2 nM (Figure S4). We fixed the concentration of streptavidin (and of Avidin or Neutravidin) in the reaction to 20 μM to be in saturation and because this concentration does not significantly affect the expression of a reporter gene (Figure S5) or of *mreB* (Figure S6). Taking a phospholipid surface area of 40−50 $Å^2$, a streptavidin protein attached to the membrane covers about 200 phospholipids; therefore, a concentration of around 1% of lipid-biotin is large enough to create a complete membrane coverage when enough streptavidin is added to the reaction. We varied the molar concentration of lipid-biotin in the membrane by taking four points: 0%, 0.33%, 1%, and 3.3%.

The deformations were characterized by the ratio L/S determined by measuring the long axis (L) and the short axis (S) of each liposome after 12 h of incubation. The L/S ratio was calculated with respect to the spherical nondeformed liposomes just after they are prepared. By definition, L/S is equal to one for a spherical object. The liposomes were binned as a function of their radius, by 2 μm increments (Figure S7), to convert the statistics into histograms that are visually easier to interpret, as described before.[30] The segment 0−2 μm, for which the deformations are the largest, is relevant to the size of *E. coli*.

As expected, MreB interacts with the bilayer in the absence of lipid-biotin in the membrane without deforming the spherical liposomes[40] (Figure 4). Deformations are observed only when lipid-biotin are added to the membrane in the presence of streptavidin in the reaction. The statistical analysis shows that deformations are the most pronounced and abundant for a molar lipid-biotin concentration of 1% (Figure 4). No deformations are observed for liposomes of radii larger than 10 μm, consistent with the persistence length of MreB filaments on the order of 10 μm.[41] We then tested avidin and neutravidin in the same conditions (20 μM), with 1% lipid-biotin in the membrane. Comparable statistics of deformation are observed (Figure 5). The case with avidin was characterized by the presence of deformed liposomes in all the sizes, although the percentage of deformations for large liposomes is small. As importantly, the statistics of deformation for the three biotin-binding proteins are similar to the statistics obtained when PE-PEG5000 is used (Figure 5). Two additional control experiments consisted of expressing *mreB* without biotin-binding protein added to the reaction with or without lipid-biotin in the membrane. In the two cases no deformations were observed (Figure S8). The polymerization of MreB at the inner membrane of the liposomes is promoted by the presence of a background of macromolecules attached to the bilayer and

https://dx.doi.org/10.1021/acs.biomac.0c00513
Biomacromolecules XXXX, XXX, XXX−XXX

independent of their nature. The macromolecules attached to the membrane create a two-dimensional excluded volume that fosters the polymerization of MreB at the inner membrane because MreB interacts spontaneously with lipids via its N-terminus end.[40] This observation supports the hypothesis that entropy is the major factor responsible for stimulating MreB polymerization and self-assembly at the membrane.

The three-dimensional reconstitution of liposomes shows the presence of long MreB filaments at the membrane and of bundles of filaments only when crowding is achieved at the membrane (Figure 6). Some large aggregates of MreB are also visible that we attribute to the strength of the system and the fact that the synthesis of MreB is not regulated and much larger than the typical concentration found in *E. coli*, on the order of 5−10 μM[42] (Figure S4). When no crowding is emulated at the membrane of the liposomes, one can observe interaction of MreB with the bilayer and the formation of a few short filaments (Figure S9).

4. CONCLUSIONS

TXTL-based synthetic cells are ideal experimental environments to isolate some of the biochemical and biophysical mechanisms used by living cells to achieve active biological functions. In this work we unraveled several important facets of membrane and cytoplasmic molecular crowding in cell-sized liposomes that are programmed genetically. While cytoplasmic crowding has proven useful to boost the efficacy of transcription and translation in test tube reactions, in a synthetic cell it is the membrane crowding that appears to be essential for self-assembly at the bilayer and sufficient to keep protein synthesis at its highest when lipid-PEGs are used. This result was unexpected for synthetic cell engineering. The PEG polymer, attached to the lipid, enables homogeneous encapsulation of the TXTL reaction in liposomes and a linear response of cell-free expression across a population of cell-sized liposomes, from 1 to 30 μm in diameter. The presence of PEG attached to the bilayer allows accelerating the polymerization of a cytoskeleton targeted to the inner membrane into a network capable of deforming spherical liposomes into rods. By demonstrating that other macromolecules attached to the membrane have the same effect on MreB self-assembly, we show that it is the presence of macromolecules attached to the membrane, independent from their nature, that promotes and accelerates the polymerization of the cytoskeleton protein MreB at the inner membrane. We anticipate that such an entropic effect of membrane crowding is essential for other cellular mechanisms located at the membrane. Adding a crowder in the cytoplasm does not improve cell-free expression or self-assembly at the bilayer when PEG-lipids are added to the membrane, which was also unanticipated.

The pros, cons, and optimum settings of the methods to emulate membrane crowding are summarized in Table 1. While using the biotin−streptavidin system offers some flexibility to produce crowding at the membrane, the lipid-PEG approach enables both optimum and uniform cell-free expression, in addition to providing biophysical conditions to promote self-assembly at the inner membrane. On a broader extent, this study shows that developing active biological functions in synthetic cells is far more complicated than just executing DNA programs. Besides the genetics, cells use a broad repertoire of molecular mechanisms that have to be deciphered to further integrate functions together into operational cell analogs.

Table 1. Emulation of Membrane Molecular Crowding in Synthetic Cells, Pros, and Cons of the Different Methods

lipid-PEGs
pros:
• optimum for cytoplasmic expression and membrane self-assembly
• easy control of the concentration at the membrane
• several sizes available (PEG moiety)
• increases the number of liposomes formed by the emulsion method
• cheap and easy to implement
cons:
• does not reproduce the diversity of proteins at the membrane
• only available for PE lipid heads
optimum conditions:
• DSPE-PEG5000:0.66% molar in membrane, no PEG in reaction
• DSPE-PEG2000:1% molar in membrane, no PEG in reaction
lipid-biotin
pros:
• good for self-assembly at the membrane
• ionic, can be positive (avidin) or negative (neutravidin, streptavidin)
• easy control of the concentration at the membrane
• strong binding not displaced by TXTL components
• cheap and easy to implement
cons:
• does not increase the yield of liposomes formed by the emulsion method
• does not improve cytoplasmic expression
optimum conditions:
• PE-biotinyl at 1% molar in membrane, 20 μM biotin-binding protein in reaction, 1.5% (1.9 mM) PEG8000 in reaction

■ ASSOCIATED CONTENT

Supporting Information

The Supporting Information is available free of charge at https://pubs.acs.org/doi/10.1021/acs.biomac.0c00513.

Figure S1, Batch mode TXTL reactions; Figure S2, Cell-free synthesis of deGFP in synthetic cells (PE-PEG2000); Figure S3, Cell-free synthesis of mCherry in synthetic cells (PE-PEG5000); Figure S4, Batch mode synthesis of MreB; Figure S5, Effect of biotin-binding proteins on the synthesis of deGFP; Figure S6, Effect of biotin-binding proteins on the synthesis of MreB; Figure S7, Scattered plot to histogram analysis; Figure S8, Control experiments for the biotin-binding proteins in synthetic cells; Figure S9, Structures formed by MreB in synthetic cells; Table S1, DNA sequences; Table S2, Root mean square end-to-end distance of PEG polymer (PDF)

■ AUTHOR INFORMATION

Corresponding Authors

Vincent Noireaux − *School of Physics and Astronomy, University of Minnesota, Minneapolis, Minnesota 55455, United States;* orcid.org/0000-0002-5213-273X; Email: noireaux@umn.edu

David Garenne − *School of Physics and Astronomy, University of Minnesota, Minneapolis, Minnesota 55455, United States;* Email: david.garenne@hotmail.fr

Complete contact information is available at: https://pubs.acs.org/10.1021/acs.biomac.0c00513

https://dx.doi.org/10.1021/acs.biomac.0c00513
Biomacromolecules XXXX, XXX, XXX−XXX

Author Contributions

D.G. and V.N. designed the research, D.G. performed the experiments, D.G. and V.N. analyzed the data, V.N. wrote the manuscript, and D.G. edited the manuscript.

Notes

The authors declare the following competing financial interest(s): The Noireaux laboratory receives research funds from Arbor Biosciences, a distributor of the myTXTL cell-free protein synthesis kit.

■ ACKNOWLEDGMENTS

V.N. acknowledges funding support from Human Frontier Science Program Grant RGP0037/2015 and the National Science Foundation Grant MCB-1613677.

■ REFERENCES

(1) Caschera, F.; Noireaux, V. Integration of Biological Parts toward the Synthesis of a Minimal Cell. *Curr. Opin. Chem. Biol.* **2014**, *22*, 85−91.
(2) Stano, P. Gene Expression Inside Liposomes: From Early Studies to Current Protocols. *Chem. - Eur. J.* **2019**, *25* (33), 7798−7814.
(3) Wu, F.; Tan, C. The Engineering of Artificial Cellular Nanosystems Using Synthetic Biology Approaches. *Wiley Interdiscip. Rev. Nanomedicine Nanobiotechnology* **2014**, *6* (4), 369−383.
(4) Oberholzer, T.; Nierhaus, K. H.; Luisi, P. L. Protein Expression in Liposomes. *Biochem. Biophys. Res. Commun.* **1999**, *261* (2), 238−241.
(5) Stano, P.; Kuruma, Y.; Souza, T. P.; Luisi, P. L. Biosynthesis of Proteins inside Liposomes. *Methods Mol. Biol.* **2010**, *606*, 127−145.
(6) Ishikawa, K.; Sato, K.; Shima, Y.; Urabe, I.; Yomo, T. Expression of a Cascading Genetic Network within Liposomes. *FEBS Lett.* **2004**, *576* (3), 387−390.
(7) Noireaux, V.; Libchaber, A. A Vesicle Bioreactor as a Step toward an Artificial Cell Assembly. *Proc. Natl. Acad. Sci. U. S. A.* **2004**, *101* (51), 17669−17674.
(8) Doerr, A.; de Reus, E.; van Nies, P.; van der Haar, M.; Wei, K.; Kattan, J.; Wahl, A.; Danelon, C. Modelling Cell-Free RNA and Protein Synthesis with Minimal Systems. *Phys. Biol.* **2019**, *16* (2), 025001.
(9) Kuruma, Y.; Stano, P.; Ueda, T.; Luisi, P. L. A Synthetic Biology Approach to the Construction of Membrane Proteins in Semi-Synthetic Minimal Cells. *Biochim. Biophys. Acta, Biomembr.* **2009**, *1788* (2), 567−574.
(10) Spencer, A. C.; Torre, P.; Mansy, S. S. The Encapsulation of Cell-Free Transcription and Translation Machinery in Vesicles for the Construction of Cellular Mimics. *J. Visualized Exp.* **2013**, *80*, No. e51304.
(11) Jia, H.; Heymann, M.; Bernhard, F.; Schwille, P.; Kai, L. Cell-Free Protein Synthesis in Micro Compartments: Building a Minimal Cell from Biobricks. *New Biotechnol.* **2017**, *39*, 199−205.
(12) Deng, N. N.; Yelleswarapu, M.; Huck, W. T. S. Monodisperse Uni- and Multicompartment Liposomes. *J. Am. Chem. Soc.* **2016**, *138* (24), 7584−7591.
(13) Schwille, P. Bottom-up Synthetic Biology: Engineering in a Tinkerer's World. *Science* **2011**, *333* (6047), 1252−1254.
(14) Solé, R. V. Evolution and Self-Assembly of Protocells. *Int. J. Biochem. Cell Biol.* **2009**, *41* (2), 274−284.
(15) Noireaux, V.; Maeda, Y. T.; Libchaber, A. Development of an Artificial Cell, from Self-Organization to Computation and Self-Reproduction. *Proc. Natl. Acad. Sci. U. S. A.* **2011**, *108* (9), 3473−3480.
(16) Garamella, J.; Majumder, S.; Liu, A. P.; Noireaux, V. An Adaptive Synthetic Cell Based on Mechanosensing, Biosensing, and Inducible Gene Circuits. *ACS Synth. Biol.* **2019**, *8* (8), 1913−1920.
(17) Majumder, S.; Garamella, J.; Wang, Y. L.; Denies, M.; Noireaux, V.; Liu, A. P. Cell-Sized Mechanosensitive and Biosensing Compartment Programmed with DNA. *Chem. Commun.* **2017**, *53* (53), 7349−7352.
(18) Garamella, J.; Marshall, R.; Rustad, M.; Noireaux, V. The All E. Coli TX-TL Toolbox 2.0: A Platform for Cell-Free Synthetic Biology. *ACS Synth. Biol.* **2016**, *5* (4), 344−355.
(19) Van Nies, P.; Westerlaken, I.; Blanken, D.; Salas, M.; Mencía, M.; Danelon, C. Self-Replication of DNA by Its Encoded Proteins in Liposome-Based Synthetic Cells. *Nat. Commun.* **2018**, *9* (1), 1583−1595.
(20) Furusato, T.; Horie, F.; Matsubayashi, H. T.; Amikura, K.; Kuruma, Y.; Ueda, T. De Novo Synthesis of Basal Bacterial Cell Division Proteins FtsZ, FtsA, and ZipA Inside Giant Vesicles. *ACS Synth. Biol.* **2018**, *7* (4), 953−961.
(21) Maeda, Y. T.; Nakadai, T.; Shin, J.; Uryu, K.; Noireaux, V.; Libchaber, A. Assembly of MreB Filaments on Liposome Membranes: A Synthetic Biology Approach. *ACS Synth. Biol.* **2012**, *1* (2), 53−59.
(22) Minton, A. P. How Can Biochemical Reactions within Cells Differ from Those in Test Tubes? *J. Cell Sci.* **2006**, *119* (14), 2863−2869.
(23) Ge, X.; Luo, D.; Xu, J. Cell-Free Protein Expression under Macromolecular Crowding Conditions. *PLoS One* **2011**, *6* (12), No. e28707.
(24) Niwa, T.; Sugimoto, R.; Watanabe, L.; Nakamura, S.; Ueda, T.; Taguchi, H. Large-Scale Analysis of Macromolecular Crowding Effects on Protein Aggregation Using a Reconstituted Cell-Free Translation System. *Front. Microbiol.* **2015**, *6*, 1113.
(25) Kai, L.; Dötsch, V.; Kaldenhoff, R.; Bernhard, F. Artificial Environments for the Co-Translational Stabilization of Cell-Free Expressed Proteins. *PLoS One* **2013**, *8* (2), No. e56637.
(26) Shin, J.; Noireaux, V. Efficient Cell-Free Expression with the Endogenous E. coli RNA Polymerase and Sigma Factor 70. *J. Biol. Eng.* **2010**, *4*, 8.
(27) Deng, N. N.; Vibhute, M. A.; Zheng, L.; Zhao, H.; Yelleswarapu, M.; Huck, W. T. S. Macromolecularly Crowded Protocells from Reversibly Shrinking Monodisperse Liposomes. *J. Am. Chem. Soc.* **2018**, *140* (24), 7399−7402.
(28) Rivas, G.; Fernandez, J. A.; Minton, A. P. Direct Observation of the Enhancement of Noncooperative Protein Self-Assembly by Macromolecular Crowding: Indefinite Linear Self-Association of Bacterial Cell Division Protein FtsZ. *Proc. Natl. Acad. Sci. U. S. A.* **2001**, *98* (6), 3150−3155.
(29) Cuneo, P.; Magri, E.; Verzola, A.; Grazi, E. Macromolecular Crowding" Is a Primary Factor in the Organization of the Cytoskeleton. *Biochem. J.* **1992**, *281* (2), 507−512.
(30) Garenne, D.; Libchaber, A.; Noireaux, V. Membrane Molecular Crowding Enhances MreB Polymerization to Shape Synthetic Cells from Spheres to Rods. *Proc. Natl. Acad. Sci. U. S. A.* **2020**, *117* (4), 1902−1909.
(31) Pautot, S.; Frisken, B. J.; Weitz, D. A. Production of Unilamellar Vesicles Using an Inverted Emulsion. *Langmuir* **2003**, *19* (7), 2870−2879.
(32) Garamella, J.; Garenne, D.; Noireaux, V. TXTL-Based Approach to Synthetic Cells. *Methods Enzymol.* **2019**, *617*, 217−239.
(33) Shin, J.; Noireaux, V. An E. coli Cell-Free Expression Toolbox: Application to Synthetic Gene Circuits and Artificial Cells. *ACS Synth. Biol.* **2012**, *1* (1), 29−41.
(34) Sun, Z. Z.; Hayes, C. A.; Shin, J.; Caschera, F.; Murray, R. M.; Noireaux, V. Protocols for Implementing an *Escherichia coli* Based TX-TL Cell-Free Expression System for Synthetic Biology. *J. Visualized Exp.* **2013**, *79*, No. e50762.
(35) Garenne, D.; Beisel, C. L.; Noireaux, V. Characterization of the All-E. Coli Transcription-Translation System MyTXTL by Mass Spectrometry. *Rapid Commun. Mass Spectrom.* **2019**, *33* (11), 1036−1048.
(36) Walde, P.; Cosentino, K.; Engel, H.; Stano, P. Giant Vesicles: Preparations and Applications. *ChemBioChem* **2010**, *11* (7), 848−865.
(37) Nourian, Z.; Danelon, C. Linking Genotype and Phenotype in Protein Synthesizing Liposomes with External Supply of Resources. *ACS Synth. Biol.* **2013**, *2* (4), 186−193.

https://dx.doi.org/10.1021/acs.biomac.0c00513
Biomacromolecules XXXX, XXX, XXX−XXX

(38) Sakamoto, R.; Noireaux, V.; Maeda, Y. T. Anomalous Scaling of Gene Expression in Confined Cell-Free Reactions. *Sci. Rep.* **2018**, *8* (1), 7374−7381.
(39) Neish, C. S.; Martin, I. L.; Henderson, R. M.; Edwardson, J. M. Direct Visualization of Ligand-Protein Interactions Using Atomic Force Microscopy. *Br. J. Pharmacol.* **2002**, *135* (8), 1943−1950.
(40) Salje, J.; van den Ent, F.; de Boer, P.; Löwe, J. Direct Membrane Binding by Bacterial Actin MreB. *Mol. Cell* **2011**, *43* (3), 478−487.
(41) Jiang, H.; Si, F.; Margolin, W.; Sun, S. X. Mechanical Control of Bacterial Cell Shape. *Biophys. J.* **2011**, *101* (2), 327−335.
(42) Jones, L. J. F.; Carballido-López, R.; Errington, J. Control of Cell Shape in Bacteria: Helical, Actin-like Filaments in Bacillus Subtilis. *Cell* **2001**, *104* (6), 913−922.

https://dx.doi.org/10.1021/acs.biomac.0c00513
Biomacromolecules XXXX, XXX, XXX−XXX

Supporting information

Analysis of cytoplasmic and membrane molecular crowding in genetically programmed synthetic cells

David Garenne and Vincent Noireaux
School of Physics and Astronomy, University of Minnesota, 115 Union Street SE, Minneapolis, MN 55455, USA

Corresponding authors:
noireaux@umn.edu
David.garenne@hotmail.fr

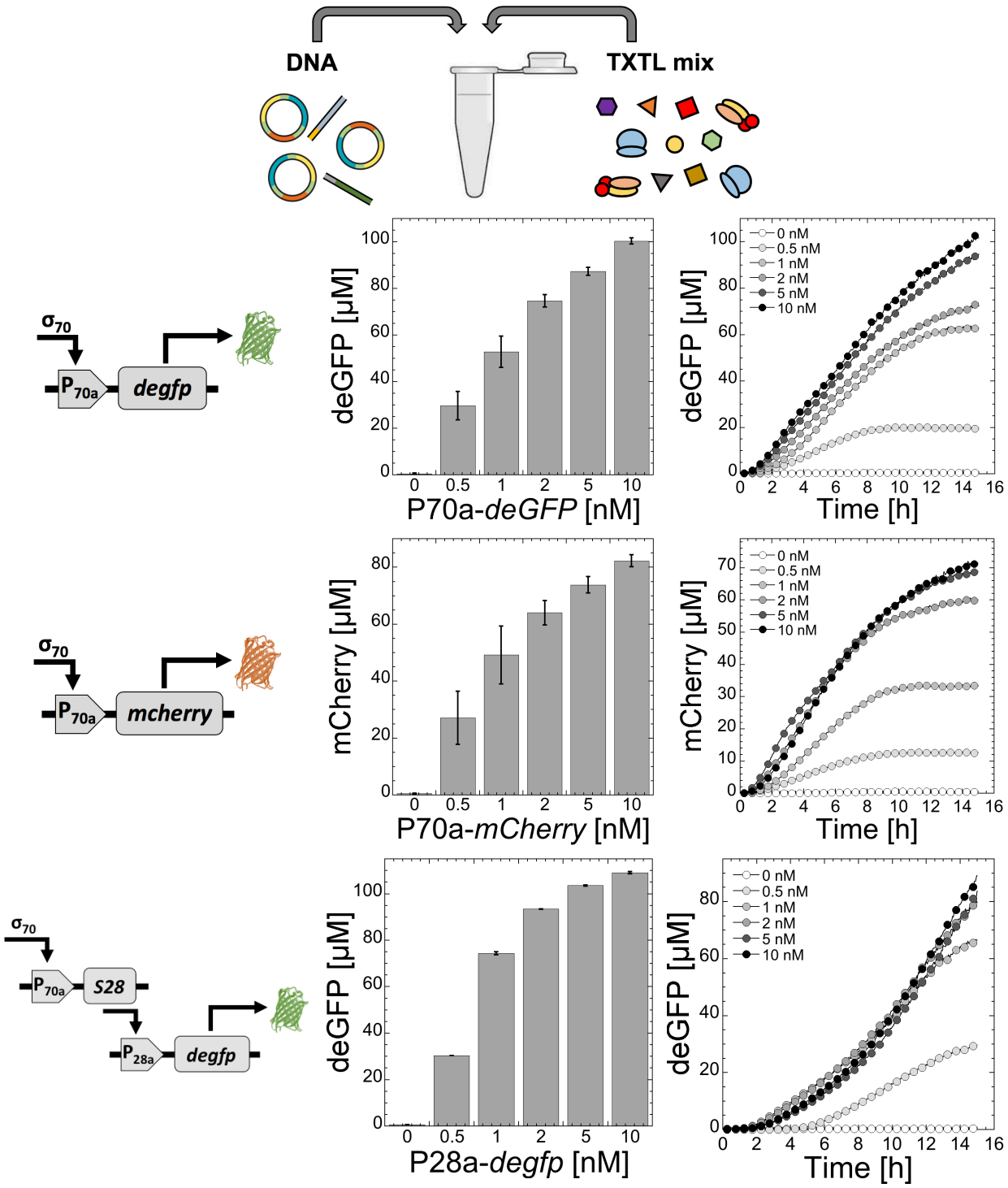

Figure S1. Batch mode TXTL reactions. **Top.** The reactions are assembled in test tubes or on well plates. **Middle rows.** Expression of *egfp* and *mcherry* through the P70a promoter, endpoint and kinetics. The P70a promoter was used to express soluble reporter proteins for the analysis of the effects of cytoplasmic molecular crowding. The shapes of the kinetics of the expression of *egfp* and *mcherry* are similar. **Bottom row.** S28 cascade (P70a-*S28* fixed at 0.5 nM) for the synthesis of deGFP, endpoints and kinetics. For the cascade, the transcription factor S28 is

continuously produced, consequently the transcription is not performed at constant polymerase concentration, which explains the constantly increasing rate of deGFP synthesis, as opposed to constant rate for P70a. The cascade S28 was used to synthesize MreB. This transcriptional activation configuration enables the expression of genes that are toxic to *E. coli* because the promoter P28a is silent, as we explained in previous publications[1,2].

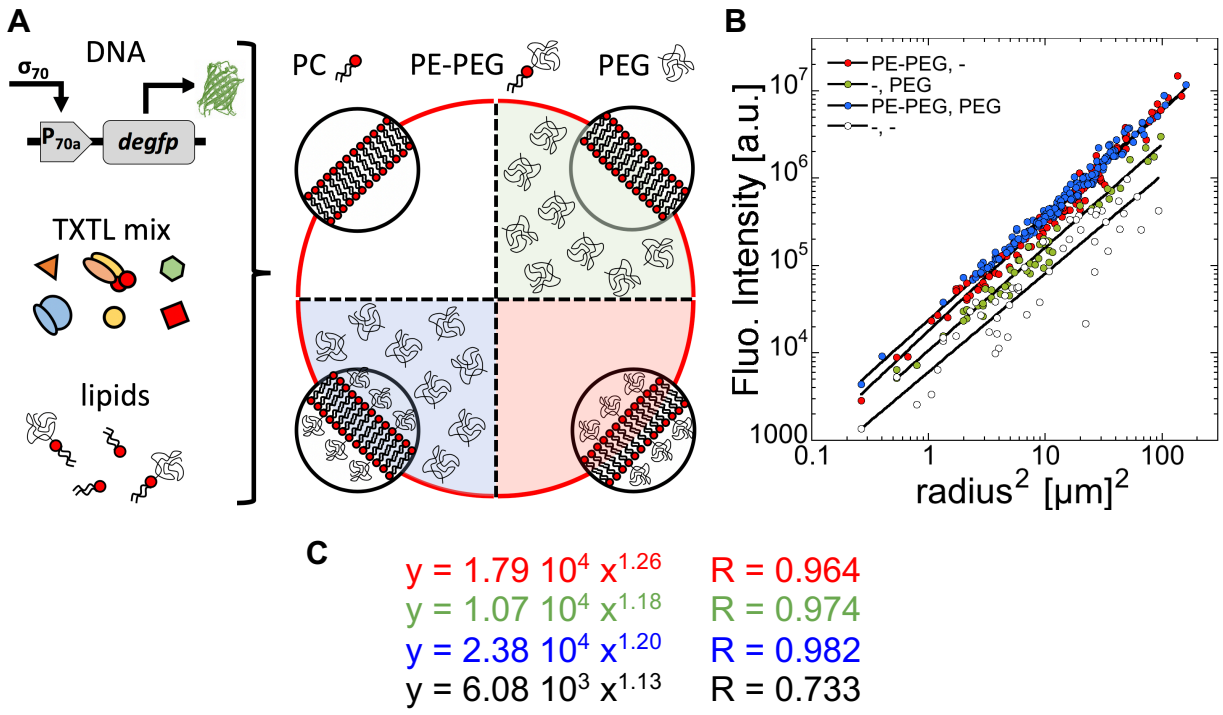

Figure S2. Cell-free expression of *degfp* in synthetic cells in the presence or absence of PEG8000 (noted PEG) in the reaction or DSPE-PEG2000 (noted PE-PEG) at the membrane. (A) The reaction components are encapsulated in cell-sized liposomes, *degfp* is expressed through the P70a constitutive promoter (plasmid P70a-*degfp*, 5 nM). Four types of liposome populations are made: with PEG and PE-PEG, with PEG only, with PE-PEG only, with none. (B) The fluorescence intensity is plotted with respect to the square of the radius of the liposomes. (C) The data are power fitted.

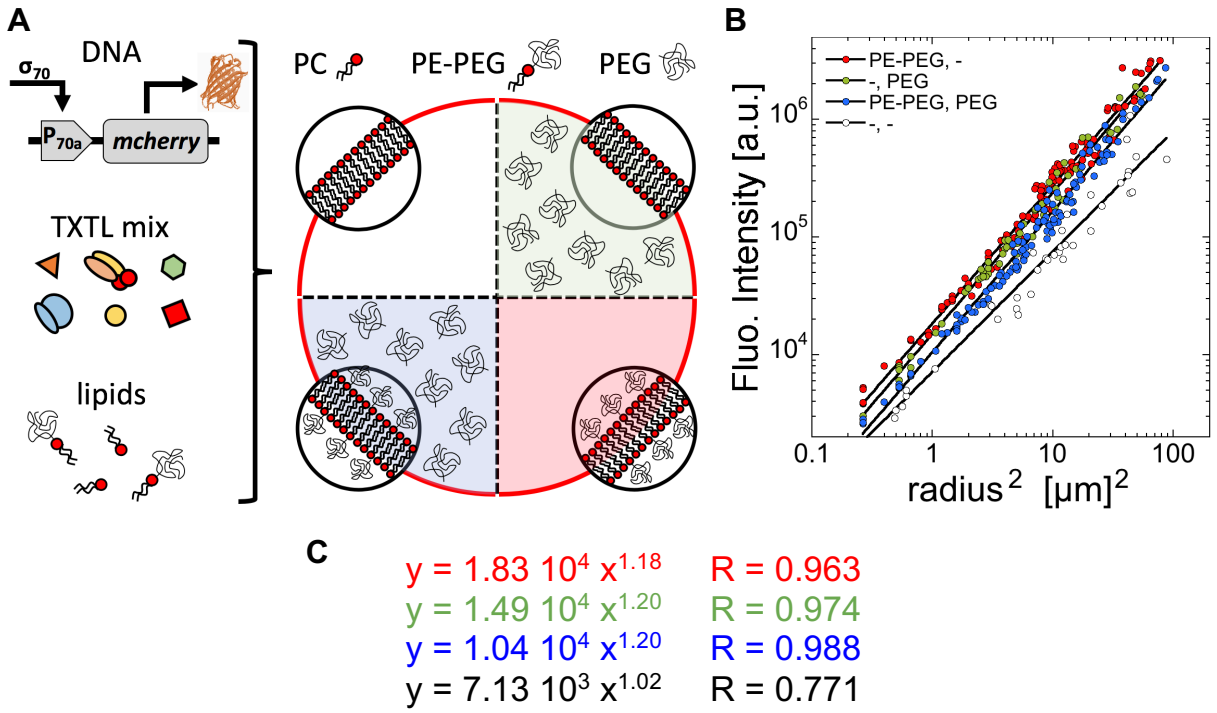

Figure S3. Cell-free expression of *mcherry* in synthetic cells in the presence or absence of PEG8000 (noted PEG) in the reaction or DSPE-PEG5000 (noted PE-PEG) at the membrane. (A) The reaction components are encapsulated in cell-sized liposomes, *mcherry* is expressed through the P70a constitutive promoter (plasmid P70a-*mcherry*, 5 nM). Four types of liposome populations are made: with PEG and PE-PEG, with PEG only, with PE-PEG only, with none. (B) The fluorescence intensity is plotted with respect to the square of the radius of the liposomes. (C) The data are power fitted.

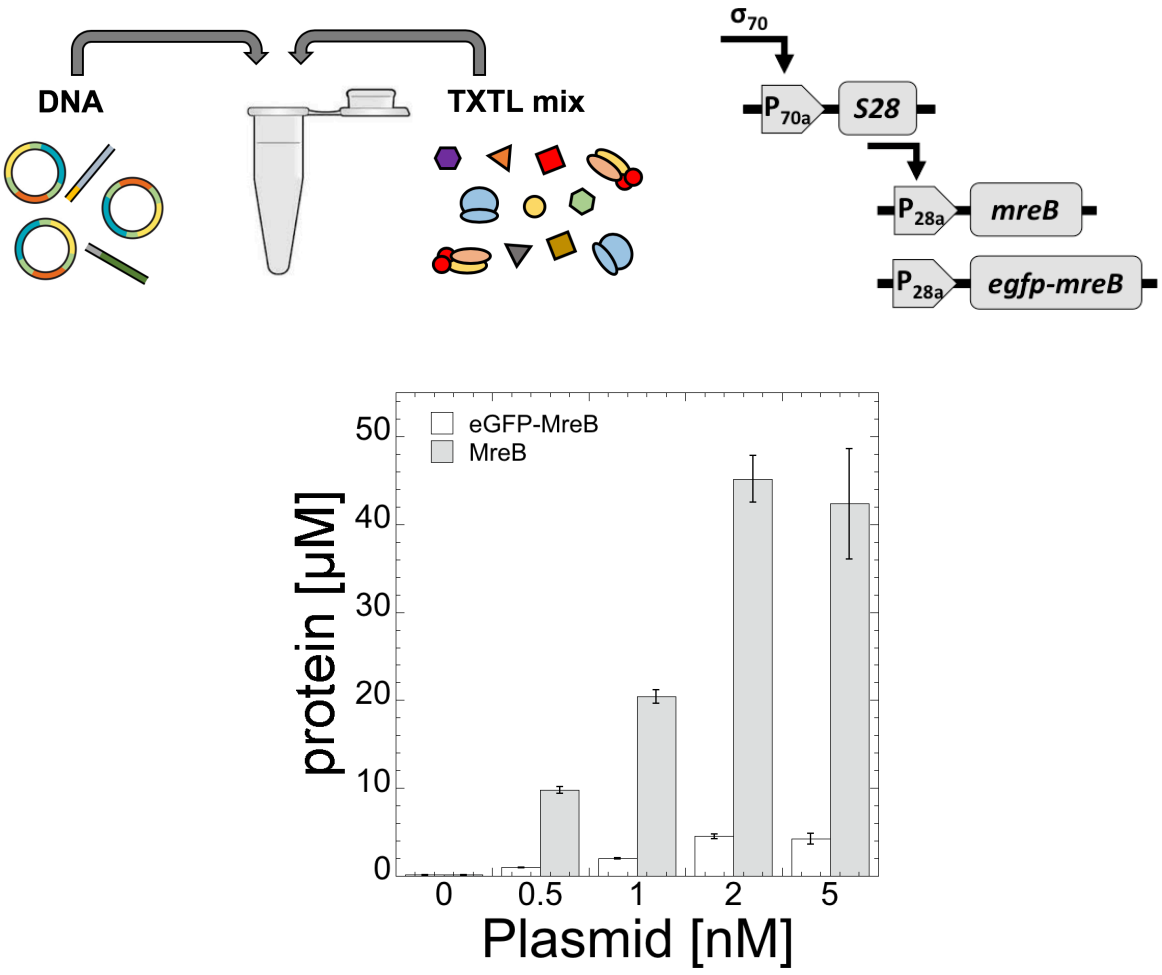

Figure S4. Batch mode TXTL reactions using the S28 transcriptional activation cascade for synthesizing MreB and eGFP-MreB. **Top.** The reaction is assembled in test tube reactions (10 μl) or on well plates (2 μl). **Bottom.** P70a-*S28* is fixed at 0.5 nM. Five combinations of the two other plasmids were tested in which the concentration of P28a-*egfp-mreB* is 10 times smaller than P28a-*mreB*: 0, 0.5, 1, 2 and 5 nM P28a-*mreB* (0, 0.05, 0.1, 0.2 and 0.5 nM P28a-*egfp-mreB*). The endpoint concentration of eGFP-MreB was measured by fluorescence, the concentration of unlabeled MreB was estimated based on the ratio of the two plasmids.

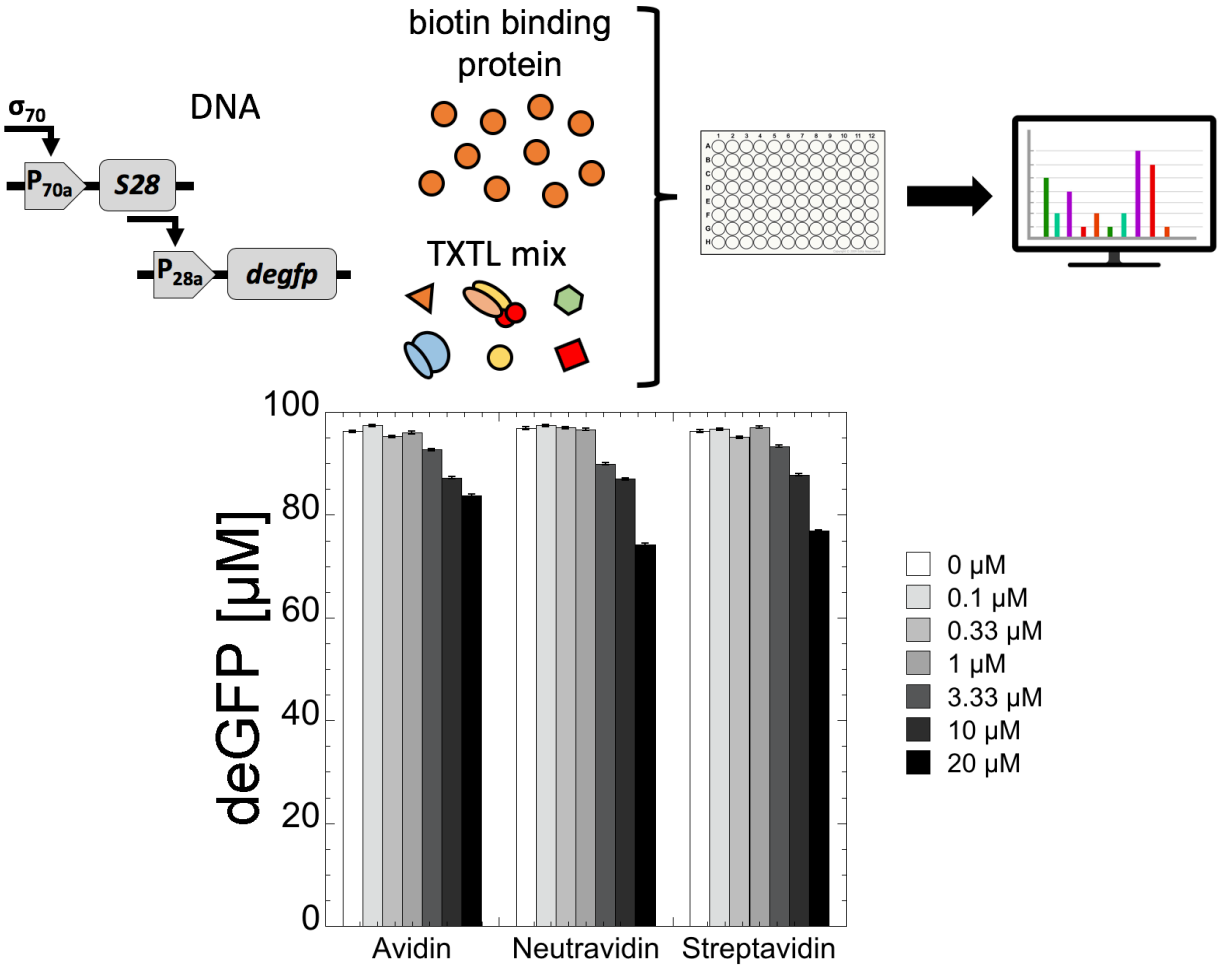

Figure S5. Effect of biotin-binding protein on the synthesis of deGFP in batch mode reactions. **Top.** Schematic of the experiment. **Bottom.** Endpoint synthesis of deGFP through the S28 cascade as a function of the concentration of either avidin, neutravidin or streptavidin added to the reaction (0.5 nM P70a-*S28*, 5 nM P28a-*degfp*).

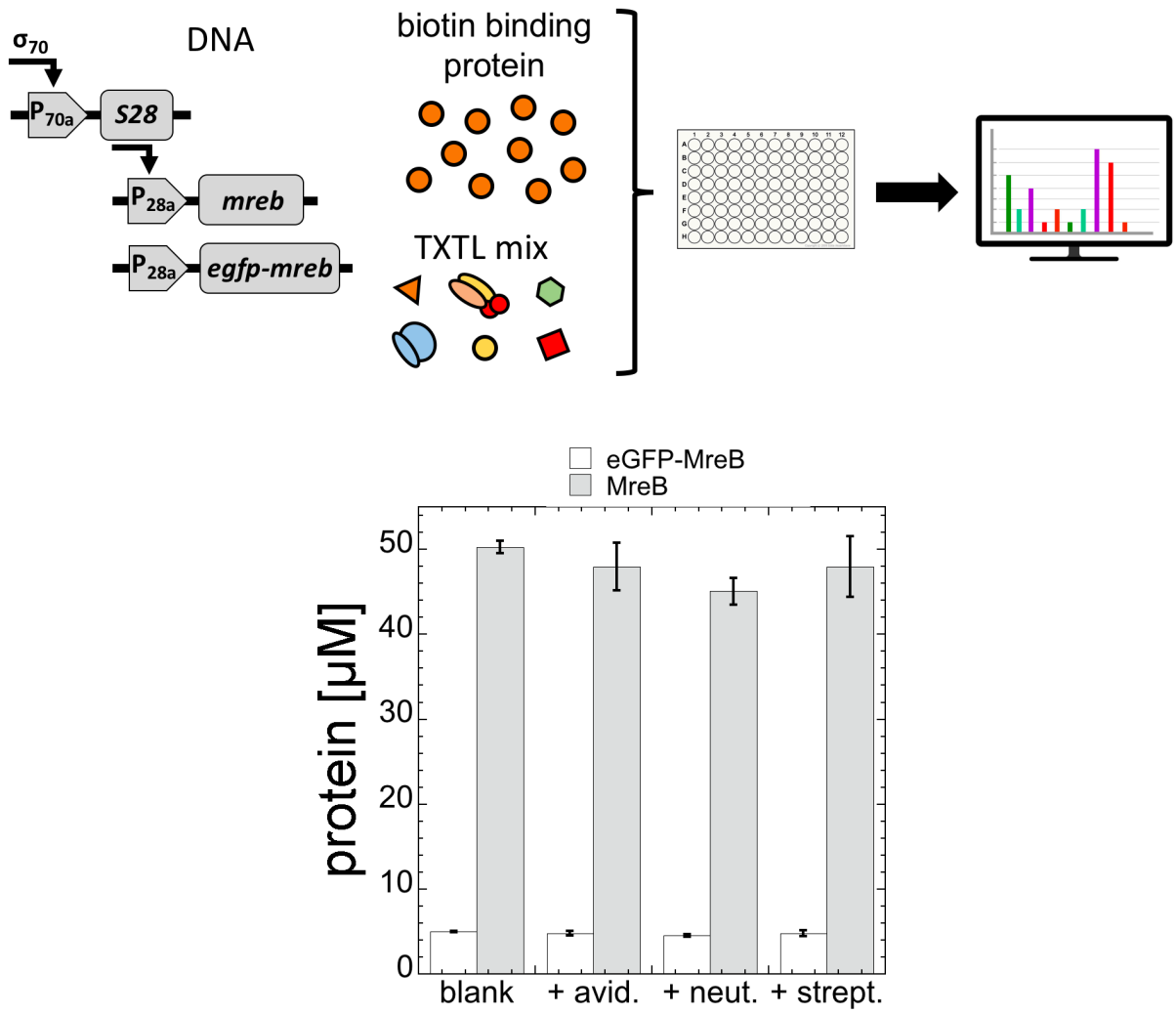

Figure S6. Effect of biotin-binding protein on the synthesis of MreB in batch mode reactions. **Top.** Schematic of the experiment. **Bottom.** Endpoint synthesis of MreB through the S28 cascade as a function of the addition of 20 μM of either avidin, neutravidin or streptavidin added to the reaction (0.5 nM P70a-*S28*, 2 nM P28a-*mreb*, 0.2 nM P28a-*egfp-mreb*).

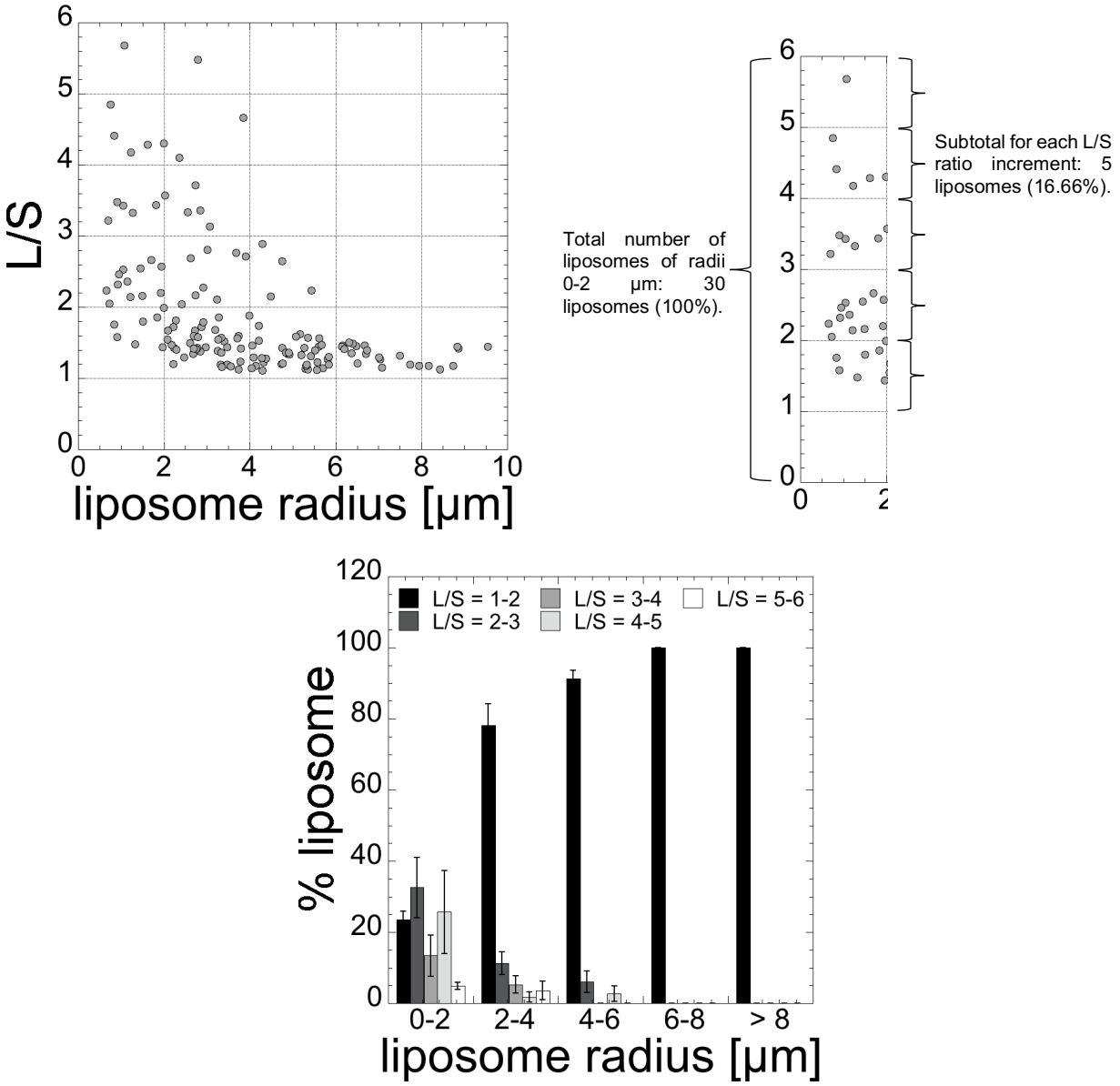

Figure S7. Data analysis of liposome deformations in the case of the synthesis of MreB into liposomes containing 0.66% of PE-PEG-5000 in the membrane. **Top left.** Scattered plot showing the ratio L/S of 149 liposomes as a function of the radius. To create histograms, the ratio L/S was binned between 1-2, 2-3, 3-4, 4-5, 5-6, the liposomes were binned according to their radii between 0-2, 2-4, 4-6, 6-8 and >8 µm. **Top right.** An example of how the histograms are created based on the scattered plot. For each 2-µm radius increment section (here we explicit the 0-2 µm radius section), the total number of liposomes is determined and represents 100% in the 0-2 µm segment. Then, for each L/S ratio increment subsection the number of liposomes is calculated and related to the total number of liposomes calculated previously. The process is repeated for 2-4 µm, 4-6 µm, 6-8 µm and >8 µm to obtain the histograms. **Bottom**. Histogram based on the top left scattered plot, in the case of PE-PEG5000 0.66% (Figure 5).

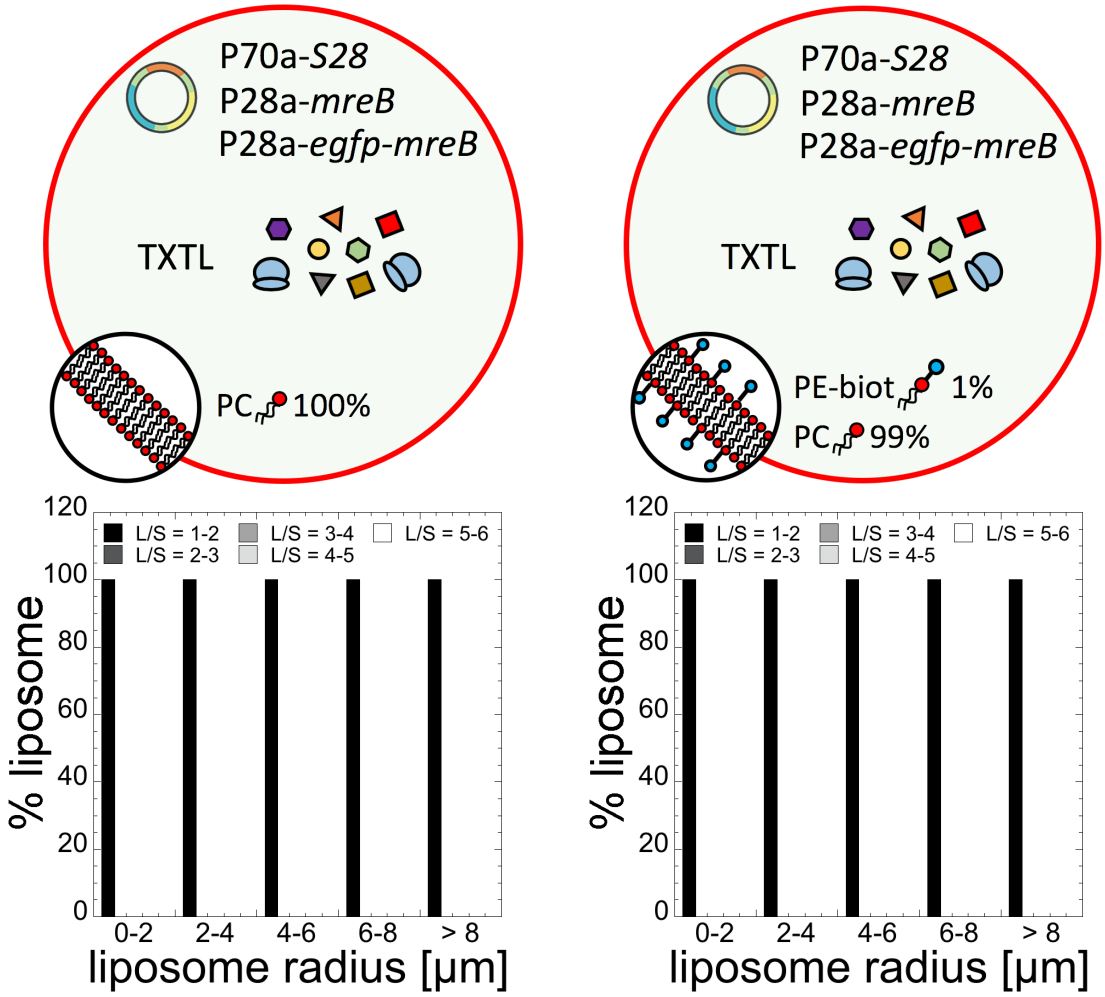

Figure S8. Statistics of liposome deformation (ratio L/S) for two control cases: no biotin-binding proteins and no lipid biotin (100% PC), and no biotin-binding protein with lipid biotin (1% molar). Plasmid concentrations: 0.5 nM P70a-*S28*, 2 nM P28a-*mreB*, 0.2 nM P28a-*egfp-mreB*. No liposome deformations were observed.

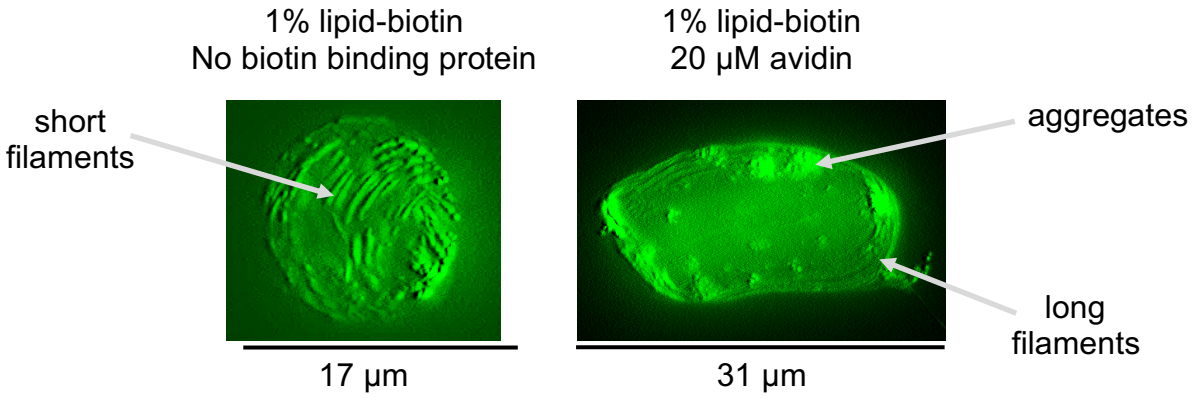

Figure S9. Excerpt from Figure 6. On the left, only short filaments are observed in the absence of membrane crowding. On the right, aggregates and long filaments are observed in the presence of membrane crowding.

The table S1 below contains the DNA sequences starting upstream the promoter and ending downstream the gene or the transcription terminator.

The promoters are highlighted in yellow.
The *degfp* (or *egfp*) reporter gene is highlighted in green.
The *mcherry* reporter gene is highlighted in red.
The other genes are highlighted in blue.
The transcription terminator is highlighted in grey.

The reporter protein deGFP is a slightly truncated version of eGFP. deGFP and eGFP have the same fluorescence properties[1,2]. The amino acid sequences of the two proteins are shown below, with in green the identical sequence:

eGFP amino acid sequence:
MSKGEELFTGVVPILVELDGDVNGHKFSVSGEGEGDATYGKLTLKFICTTGKLPVPWPTLVTTL
TYGVQCFSRYPDHMKQHDFFKSAMPEGYVQERTIFFKDDGNYKTRAEVKFEGDTLVNRIELKG
IDFKEDGNILGHKLEYNYNSHNVYIMADKQKNGIKVNFKIRHNIEDGSVQLADHYQQNTPIGDGP
VLLPDNHYLSTQSALSKDPNEKRDHMVLLEFVTAAGITHGMDELYK

deGFP amino acid sequence:
MELFTGVVPILVELDGDVNGHKFSVSGEGEGDATYGKLTLKFICTTGKLPVPWPTLVTTLTYGV
QCFSRYPDHMKQHDFFKSAMPEGYVQERTIFFKDDGNYKTRAEVKFEGDTLVNRIELKGIDFK
EDGNILGHKLEYNYNSHNVYIMADKQKNGIKVNFKIRHNIEDGSVQLADHYQQNTPIGDGPVLL
PDNHYLSTQSALSKDPNEKRDHMVLLEFVTAAGI

The reporter protein mCherry has the same amino acid sequence as mCherry, but the gene contains two silent mutations in the 5' end, that makes the gene more translatable in TXTL.

P70a-*degfp*
gcatgctgagctaacaccgtgcgtgttgacaattttacctctggcggtgataatggttgcagctagcaataattttgtttaactttaagaa ggagatataccatggagcttttcactggcgttgttcccatcctggtcgagctggacggcgacgtaaacggccacaagttcagcgtgt ccggcgagggcgagggcgatgccacctacggcaagctgaccctgaagttcatctgcaccaccggcaagctgcccgtgccctgg cccaccctcgtgaccaccctgacctacggcgtgcagtgcttcagccgctaccccgaccacatgaagcagcacgacttcttcaagt ccgccatgcccgaaggctacgtccaggagcgcaccatcttcttcaaggacgacggcaactacaagacccgcgccgaggtgaa gttcgagggcgacaccctggtgaaccgcatcgagctgaagggcatcgacttcaaggaggacggcaacatcctggggcacaag ctggagtacaactacaacagccacaacgtctatatcatggccgacaagcagaagaacggcatcaaggtgaacttcaagatccg ccacaacatcgaggacggcagcgtgcagctcgccgaccactaccagcagaacaccccatcggcgacggccccgtgctgctg cccgacaaccactacctgagcacccagtccgccctgagcaaagaccccaacgagaagcgcgatcacatggtcctgctggagtt cgtgaccgccgccgggatctaactcgagcaaagcccgccgaaaggcgggcttttctgtgtcgac
P70a-*mcherry*
gcatgctgagctaacaccgtgcgtgttgacaattttacctctggcggtgataatggttgcagctagcaataattttgtttaactttaagaa ggagatataccatggtgagcaagggcgaagaagataacatggccatcatcaaggagttcatgcgcttcaaggtgcacatggag ggctccgtgaacggccacgagttcgagatcgagggcgagggcgagggccgcccctacgagggcacccagaccgccaagct gaaggtgaccaagggtggccccctgcccttcgcctgggacatcctgtcccctcagttcatgtacggctccaaggcctacgtgaagc accccgccgacatccccgactacttgaagctgtccttccccgagggcttcaagtgggagcgcgtgatgaacttcgaggacggcg gcgtggtgaccgtgacccaggactcctccctgcaggacggcgagttcatctacaaggtgaagctgcgcggcaccaacttcccctc cgacggccccgtaatgcagaagaagaccatgggctgggaggcctcctccgagcggatgtaccccgaggacggcgccctgaa gggcgagatcaagcagaggctgaagctgaaggacggcggccactacgacgctgaggtcaagaccacctacaaggccaaga agcccgtgcagctgcccggcgcctacaacgtcaacatcaagttggacatcacctcccacaacgaggactacaccatcgtggaa cagtacgaacgcgccgagggccgccactccaccggcggcatggacgagctgtacaagtaactcgagcaaagcccgccgaaa aggcgggcttttctgtgtcgac

P70a-*S28*
gcatgctgagctaacaccgtgcgtgttgacaattttacctctggcggtgataatggttgcagctagcaataattttgtttaactttaagaa ggaggatccaaatgaattcactctataccgctgaaggtgtaatggataaacactcgctgtggcagcgttatgtcccgctggtgcgtc acgaagcattgcgcctgcaggttcgactgcccgcgagcgtggaacttgacgatctgctacaggcgggcggcattgggttacttaat gccgtcgaacgctatgacgccctacaaggaacggcatttacaacttacgcagtgcagcgtatccgtggcgctatgctggatgaact tcgcagccgtgactgggtgccgcgcagcgtgcgacgcaacgcgcgtgaagtggcacaggcaatagggcaactggagcagga acttggccgcaacgccacggaaactgaggtagcggaacgtttagggatcgatattgccgattatcgccaaatgttgctcgacacc aataacagccagctcttctcctacgatgagtggcgcgaagagcacggcgatagcatcgaactggttactgatgatcatcagcgag aaaacccgctacaacaactactggacagtaatctgcgccagcgggtgatggaagccatcgaaacgttgccggagcgcgaaaa actggtattaaccctctattaccaggaagagctgaatctcaaagagattggcgcggtgctggaggtcggggaatcgcgggtcagt cagttacacagccaggctattaaacggttacgcactaaactgggtaagttataatctagaggcgccactcgagagtcgaccaaag cccgccgaaaggcgggcttttctgtgccggc
P28a-*degfp*
cccggccaagcttcaataaagtttccccctccttgccgataacgagatcaagctagcaataattttgtttaactttaagaaggagat ataccatggagcttttcactggcgttgttcccatcctggtcgagctggacggcgacgtaaacggccacaagttcagcgtgtccggcg agggcgagggcgatgccacctacggcaagctgaccctgaagttcatctgcaccaccggcaagctgcccgtgccctggcccacc ctcgtgaccaccctgacctacggcgtgcagtgcttcagccgctaccccgaccacatgaagcagcacgacttcttcaagtccgccat gcccgaaggctacgtccaggagcgcaccatcttcttcaaggacgacggcaactacaagacccgcgccgaggtgaagttcgag ggcgacaccctggtgaaccgcatcgagctgaagggcatcgacttcaaggaggacggcaacatcctggggcacaagctggagt acaactacaacagccacaacgtctatatcatggccgacaagcagaagaacggcatcaaggtgaacttcaagatccgccacaa catcgaggacggcagcgtgcagctcgccgaccactaccagcagaacaccccatcggcgacggccccgtgctgctgcccgac aaccactacctgagcacccagtccgccctgagcaaagaccccaacgagaagcgcgatcacatggtcctgctggagttcgtgac cgccgccgggatctaactcgagcaaagcccgccgaaaggcgggcttttctgtgtcgac
P28a-*mreB*
cccggccaagcttcaataaagtttccccctccttgccgataacgagatcaagctagcaataattttgtttaactttaagaaggagat atctagaatgttgaaaaaatttcgtggcatgttttccaatgacttgtccattgacctgggtactgcgaataccctcatttatgtaaaagga caaggcatcgtattgaatgagccttccgtggtggccattcgtcaggatcgtgccggttcaccgaaaagcgtagctgcagtaggtcat gacgcgaagcagatgctgggccgtacgccgggcaatattgctgccattcgcccaatgaaagacggcgttatcgccgacttcttcgt gactgaaaaaatgctccagcacttcatcaaacaagtgcacagcaacagctttatgcgtccaagcccgcgcgttctggtttgtgtgcc ggttggcgcgacccaggttgaacgccgcgcaattcgtgaatccgcgcagggcgctggtgcccgtgaagtcttcctgattgaagaa ccgatggctgccgcaattggtgctggcctgccggtttctgaagcgaccggttctatggtggttgatatcggtggtggtaccactgaagt tgctgttatctccttgaacggtgtggtttactcctcttctgtgcgcattggtggtgaccgtttcgacgaagctatcatcaactatgtgcgtcg taattacggttctctgatcggtgaagccaccgcagaacgtatcaagcacgaaatcggttcggcttatccgggcgatgaagtccgtg aaatcgaagttcgtggccgtaacctggcagaaggtgttccacgcggttttaccctgaactccaatgaaatcctcgaagcactgcag gaaccgctgaccggtattgtgagcgcggtaatggttgcactggaacagtgcccgccggaactggcttccgacatctccgagcgcg gcatggtgctcaccggtggtggcgcactgctgcgtaaccttgaccgtttgttaatggaagaaaccggcattccagtcgttgttgctga agacccgctgacctgtgtggcgcgcggtggcggcaaagcgctggaaatgatcgacatgcacggcggcgacctgttcagcgaa gagtaaggatcctcgagcaaagcccgccgaaaggcgggcttttctgtgtcgac
P28a-*egfp-mreB*
cccggccaagcttcaataaagtttccccctccttgccgataacgagatcaagctagcaataattttgtttaactttaagaaggagat actcgaccatgagtaaaggagaagaacttttcactggagttgtcccaattcttgttgaattagatggtgatgttaatgggcacaaatttt ctgtcagtggagagggtgaaggtgatgcaacatacggaaaacttacccttaaatttatttgcactactggaaaactacctgttccatg gccaacacttgtcactactctcacttatggtgttcaatgcttttcaagatacccagatcacatgaaacagcatgacttttcaagagtgc catgcccgaaggttatgtacaggaaagaactatatttttcaaagatgacgggaactacaagacacgtgctgaagtcaagtttgaag gtgataccttgttaatagaatcgagttaaaaggtattgattttaaagaagatggaaacattcttggacacaaattggaatacaactat aactcacacaatgtatacatcatggcagacaaacaaaagaatggaatcaaagttaacttcaaaattagacacaacattgaagat ggaagcgttcaactagcagaccattatcaacaaaatactccaattggcgatggccctgtccttttaccagacaaccattacctgtcc acacaatctgccctttcgaaagatcccaacgaaaagagagaccacatggtccttcttgagtttgtaacagctgctgggattacacat ggcatggatgaactatacaaatctagaatgttgaaaaaatttcgtggcatgttttccaatgacttgtccattgacctgggtactgcgaat accctcatttatgtaaaaggacaaggcatcgtattgaatgagccttccgtggtggccattcgtcaggatcgtgccggttcaccgaaa

agcgtagctgcagtaggtcatgacgcgaagcagatgctgggccgtacgccgggcaatattgctgccattcgcccaatgaaagac
ggcgttatcgccgacttcttcgtgactgaaaaaatgctccagcacttcatcaaacaagtgcacagcaacagctttatgcgtccaagc
ccgcgcgttctggtttgtgtgccggttggcgcgacccaggttgaacgccgcgcaattcgtgaatccgcgcagggcgctggtgcccg
tgaagtcttcctgattgaagaaccgatggctgccgcaattggtgctggcctgccggtttctgaagcgaccggttctatggtggttgatat
cggtggtggtaccactgaagttgctgttatctccttgaacggtgtggtttactcctcttctgtgcgcattggtggtgaccgtttcgacgaag
ctatcatcaactatgtgcgtcgtaattacggttctctgatcggtgaagccaccgcagaacgtatcaagcacgaaatcggttcggctta
tccgggcgatgaagtccgtgaaatcgaagttcgtggccgtaacctggcagaaggtgttccacgcggttttaccctgaactccaatg
aaatcctcgaagcactgcaggaaccgctgaccggtattgtgagcgcggtaatggttgcactggaacagtgcccgccggaactgg
cttccgacatctccgagcgcggcatggtgctcaccggtggtggcgcactgctgcgtaaccttgaccgtttgttaatggaagaaaccg
gcattccagtcgttgttgctgaagacccgctgacctgtgtggcgcgcggtggcggcaaagcgctggaaatgatcgacatgcacgg
cggcgacctgttcagcgaagagtaaggatcctcgagcaaagcccgccgaaaggcgggcttttctgtgtcgac

Table S1. DNA sequences of the constructions used in this work.

The size R of an ideal polymer chain is defined as the root mean square end-to-end distance:

$$R = bN^{1/2} \text{ where :}$$

- b is the length of the effective segment ($b = 2\ L_p$, where L_p is the persistence length).
- N is the number of effective segments.

For PEG, the persistence length has been estimated to 3.8 Å[3,4]. The chemical monomer is made of three single covalent bonds, each of size 1.2-1.5 Å, therefore similar to the persistence length. The PEG monomer has a molar mass of 44 g/mol.

For a PEG of mass 5000 g/mol and a phospholipid average surface area of 40-50 $Å^2$, we find that a PG molecule covers about 65-80 phospholipids. Consequently, at a molar concentration of DSPE-PEG5000 greater than a few percent (~1-2%), the polymer covers the whole membrane. In our previous study[5], we determined that the optimum concentrations in the membrane are 0.66% for the PE-PEG5000 and 1% for the PE-PEG2000.

Lipid	n	N	R (nm)
DSPE-PEG2000	45	23	3.6
DSPE-PEG5000	114	57	5.7

Table S2. Number of chemical monomers (n), of effective segments (N) and root mean square end-to-end distance (R) for the PE-PEGs used in this work.

References

(1) Shin Noireaux, V., J. An E. Coli Cell-Free Expression Toolbox: Application to Synthetic Gene Circuits and Artificial Cells. *ACS Synth. Biol.* **2011**, *1* (1), 29–41. https://doi.org/10.1021/sb200016s.

(2) Garamella, J.; Marshall, R.; Rustad, M.; Noireaux, V. The All E. Coli TX-TL Toolbox 2.0: A Platform for Cell-Free Synthetic Biology. *ACS Synth. Biol.* **2016**, *5* (4), 344-355. https://doi.org/10.1021/acssynbio.5b00296.

(3) Kienberger, F.; Pastushenko, V. P.; Kada, G.; Gruber, H. J.; Riener, C.; Schindler, H.; Hinterdorfer, P. Static and Dynamical Properties of Single Poly(Ethylene Glycol) Molecules Investigated by Force Spectroscopy. *Single Mol.* **2000**, *2*, 123-128. https://doi.org/10.1002/1438-5171(200006)1:2<123::AID-SIMO123>3.0.CO;2-3.

(4) Lee, H.; Venable, R. M.; MacKerell, A. D.; Pastor, R. W. Molecular Dynamics Studies of Polyethylene Oxide and Polyethylene Glycol: Hydrodynamic Radius and Shape Anisotropy. *Biophys. J.* **2008**, *95* (4), 1590-1599. https://doi.org/10.1529/biophysj.108.133025.

(5) Garenne, D.; Libchaber, A.; Noireaux, V. Membrane Molecular Crowding Enhances MreB Polymerization to Shape Synthetic Cells from Spheres to Rods. *Proc. Natl. Acad. Sci. U. S. A.* **2020**, *117* (4), 19021909. https://doi.org/10.1073/pnas.1914656117.